Tensor Network 2023@筑波大学計算科学研究センター
2023/11/15 13:00 ~ 14:15

量子多体計算（物性/統計/化学...）に焦点を当てた

量子計算に対するテンソルネットワーク法の応用

上田宏[A,B]
[A]阪大QIQB，　[B]理研R-CCS

Quantum many-body physics in condensed matter physics

Various applications

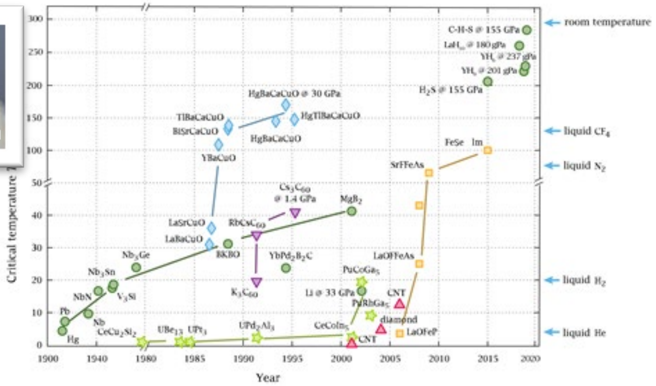

https://www.chemistryworld.com/news/room-temperature-superconductivity-finally-claimed-by-mystery-material/4012591.article

Superconductor

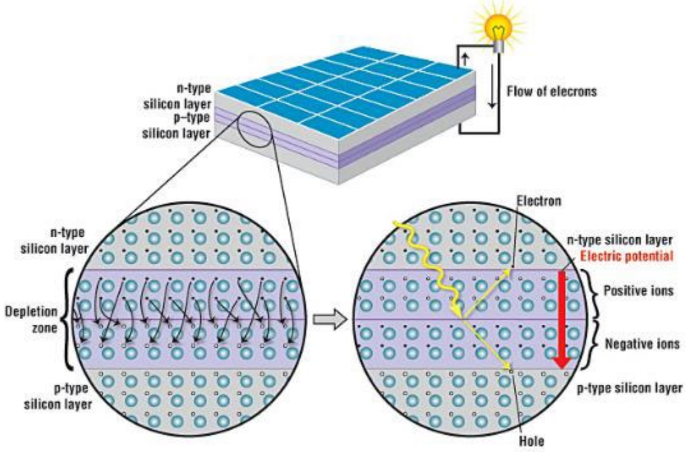

https://www.acs.org/education/resources/highschool/chemmatters/past-issues/archive-2013-2014/how-a-solar-cell-works.html

Solar cell

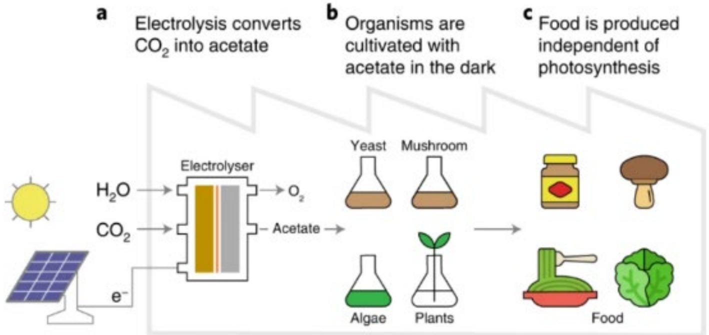

Nature Food **3**, 461–471 (2022).

Artificial photosynthesis

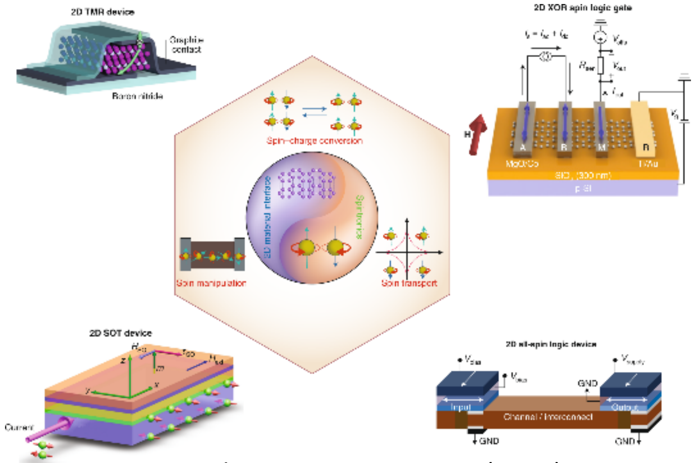

Nature Electronics **2**, 274–283 (2019).

Spintronics

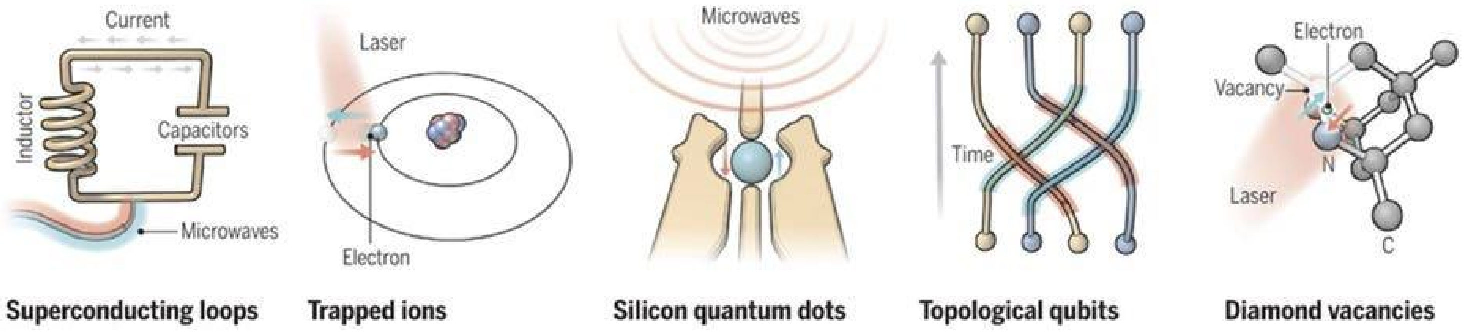

https://www.forbes.com/sites/moorinsights/2019/09/16/quantum-computer-battle-royale-upstart-ions-versus-old-guard-superconductors/?sh=2fcebae32cb8

Quantum computer

Quantum Lattice Model

(Time independent) Schrödinger equation $H|\Psi\rangle = E_\Psi|\Psi\rangle$

- Quantum spin systems（XXZ model)

$$H = \sum_{\langle i,j\rangle} \left[J^{xy}\left(s_i^x s_j^x + s_i^y s_j^y\right) + J^z s_i^z s_j^z\right]$$

- Hubbard model (Fermion/Boson)

$$H = -t\sum_{\sigma\langle i,j\rangle} c_{i\sigma}^\dagger c_{j\sigma} + U\sum_i n_{i\uparrow} n_{i\downarrow}$$

- Kitaev model under the magnetic field

$$H = -\sum_\gamma \sum_{\langle i,j\rangle_\gamma} J_\gamma s_i^\gamma s_j^\gamma - \boldsymbol{h}\cdot\sum_i \boldsymbol{s}_i$$

Etc…

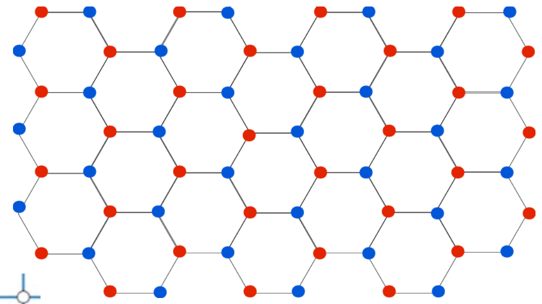

Honeycomb Lattice

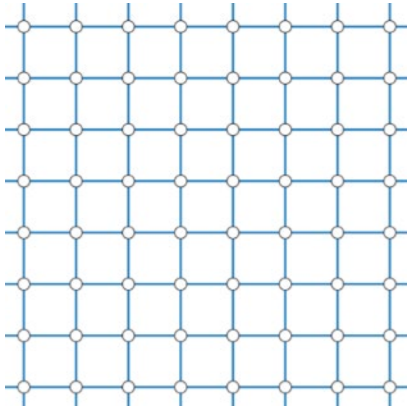

Square Lattice

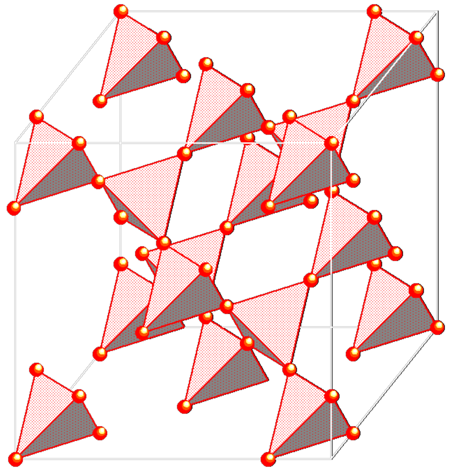

Pyrochlore Lattice

Goal of Quantum Software (QS)

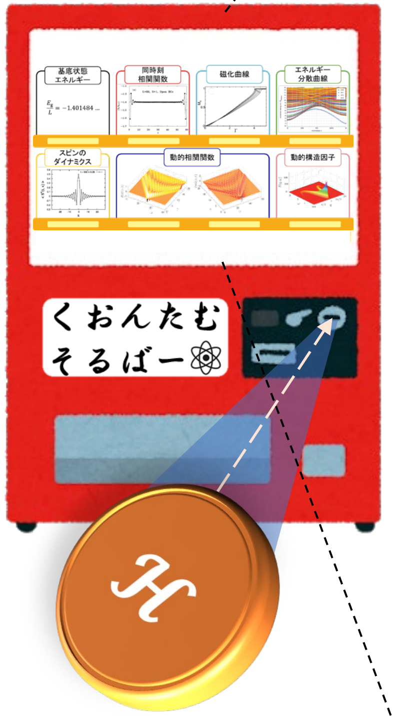

Hamiltonian of $S = 1$ Heisenberg spin chain

Ground-state energy

$$\frac{E_g}{N} = -1.401484 \ldots$$

Correlation functions

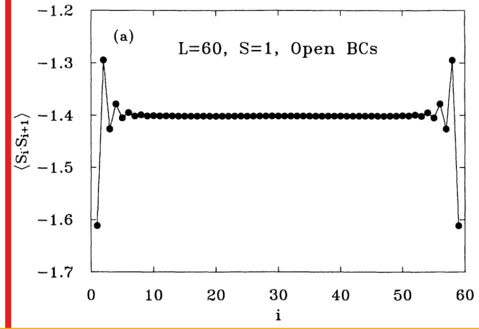

Magnetization curve

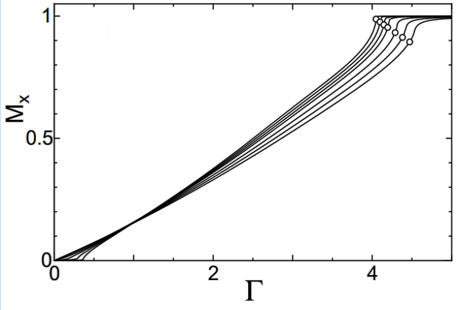

Energy dispersion

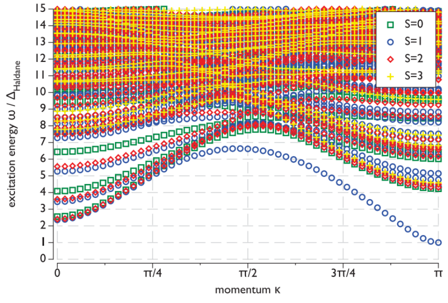

Real-time evolution

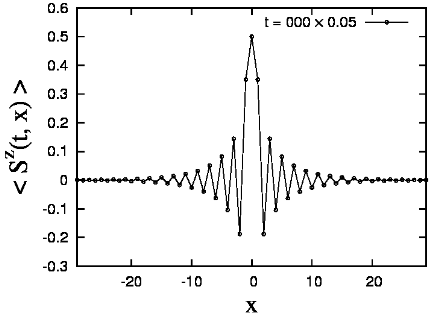

Dynamical correlation functions / structure factor

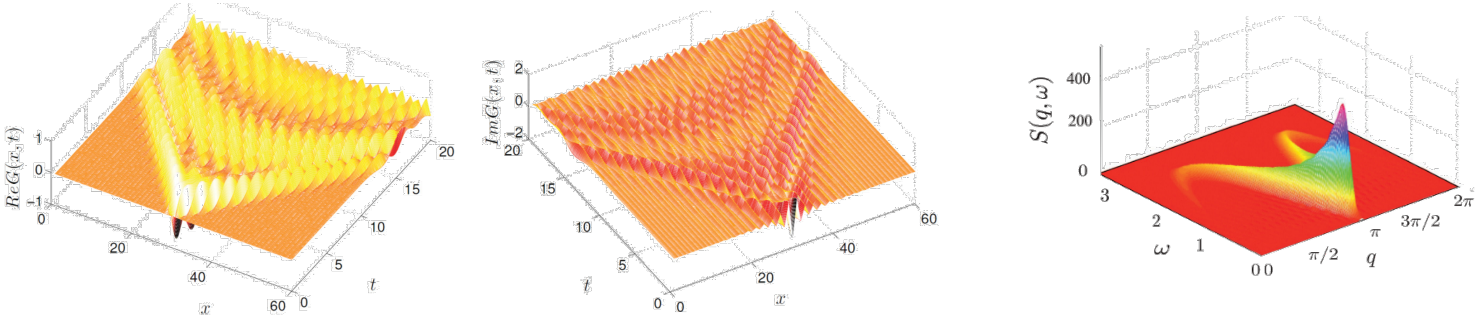

Refs. : PRB **48**, 3844 (1993); PRB **48**, 10345 (1993); PRB **64**, 224422 (2001); PRB **85**, 100408(R) (2012); PRB **86**, 245107 (2012).

Limitations with Classical Computing

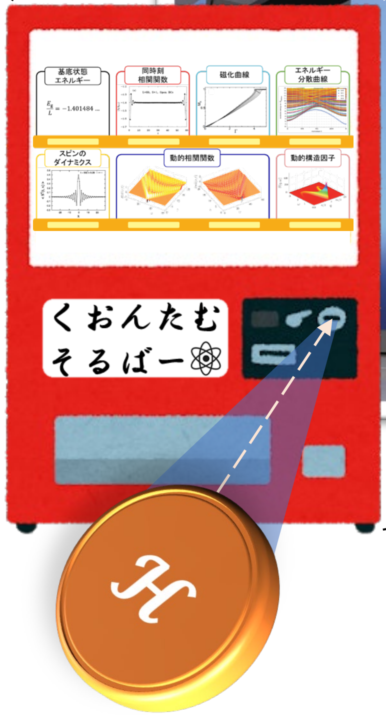

Numerical Diagonalization

- Numerically exact
- Numerical cost: $\mathcal{O}(\exp(N))$

48-qubit simulation with K

Comput. Phys. Commun. **237**, 47 (2019)

Variational approach

Numerical cost: $\mathcal{O}(\mathrm{poly}(N))$

Numerical accuracy: Highly dependent

Expectations

Solver utilizing D.O.F of quantum computer (QC)

QC from Osaka Univ. ➔

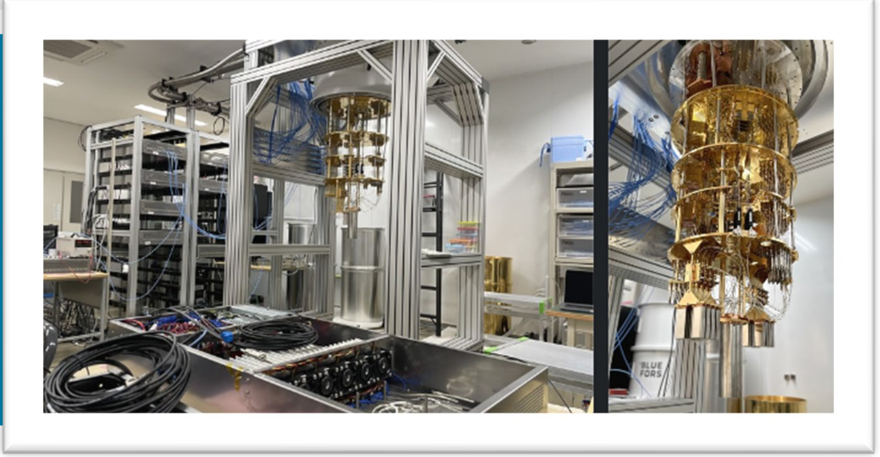

Roadmap of Quantum computer

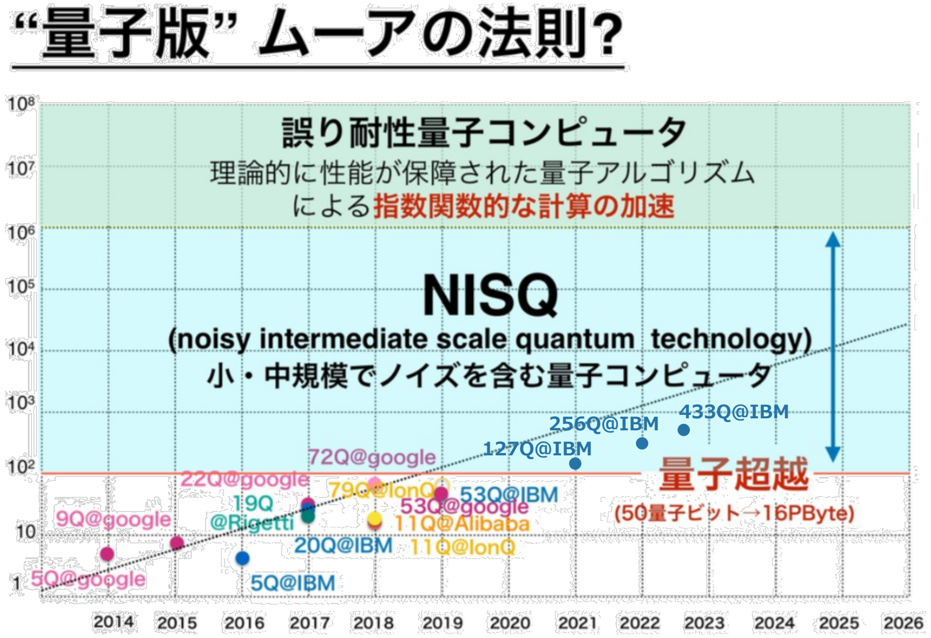

Slide presented by Prof. Fujii @ Osaka Univ. （2019/11/20）+α
https://research.ibm.com/blog/quantum-volume-256

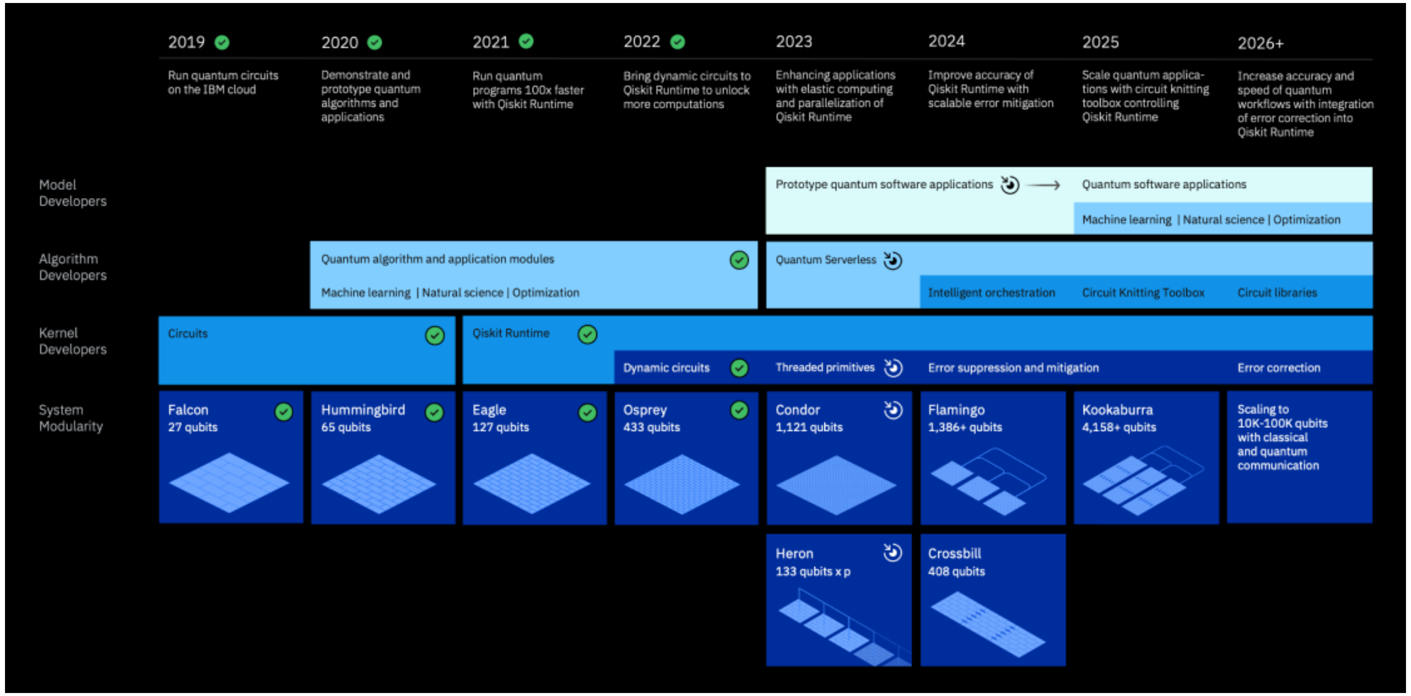

https://www.ibm.com/quantum/roadmap

Expected Application

- Security: Prime factorization, Network, Cloud computing, Money, Certification, …
- AI & Data Science: Database, Matrix inversion, Machine learning, …
- Material Science: Quantum chemistry, Drug discovery, …
- **Fundamental Science: New phase of matter, High-Tc Superconductivity, Black hole, …**

Quantum supremacy

Google team: Nature 574, 505 (Oct. 24, 2019)

53(54) qubits

Random quantum circuit

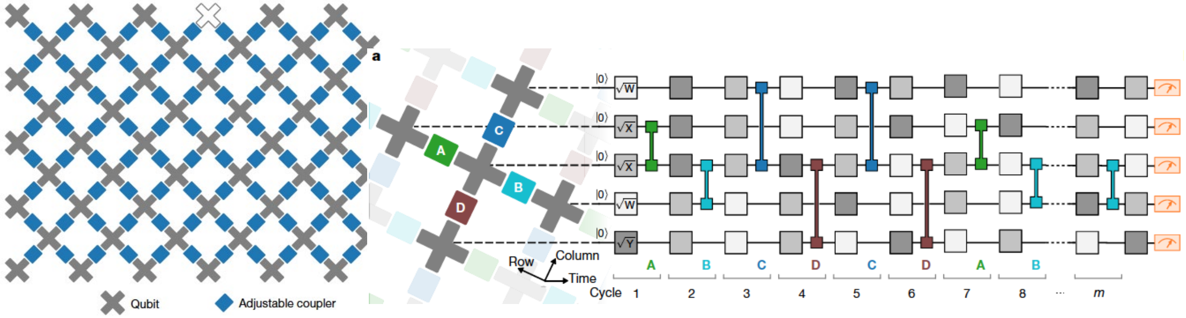

200 Sec.

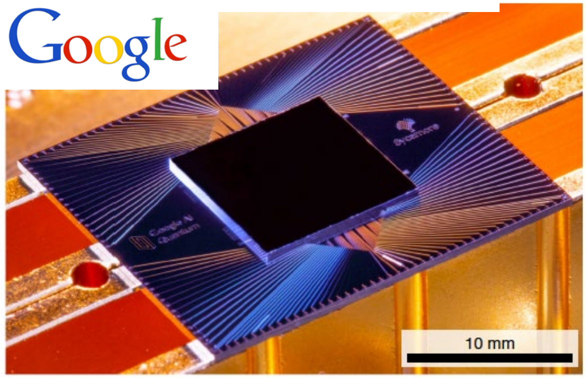

vs.

1,000 Year

(2.5 day, IBM team)

The world's fastest supercomputer at the time.

Tensor network method (MPS)

Y. Zhou, M. Stoudenmire & X. Waintal, Phys. Rev. X **10**, 041038 (2020).

- Simulations (54 qubits, 20 layers) equivalent to or better than Google's experiments (overall fidelity > 99.8%) can be performed in a few hours on a laptop.

Tensor-network based classical simulation

C. Huang, et al., arXiv:2005.06787
Y. Liu, et al., arXiv:2110.14502.

- Perform numerically exact tensor contraction
- Using a Summit-grade supercomputer

1000 year ➔ 304 sec.

Quantum supremacy

Google Quantum AI and Collaborators, arXiv: 2304.11119

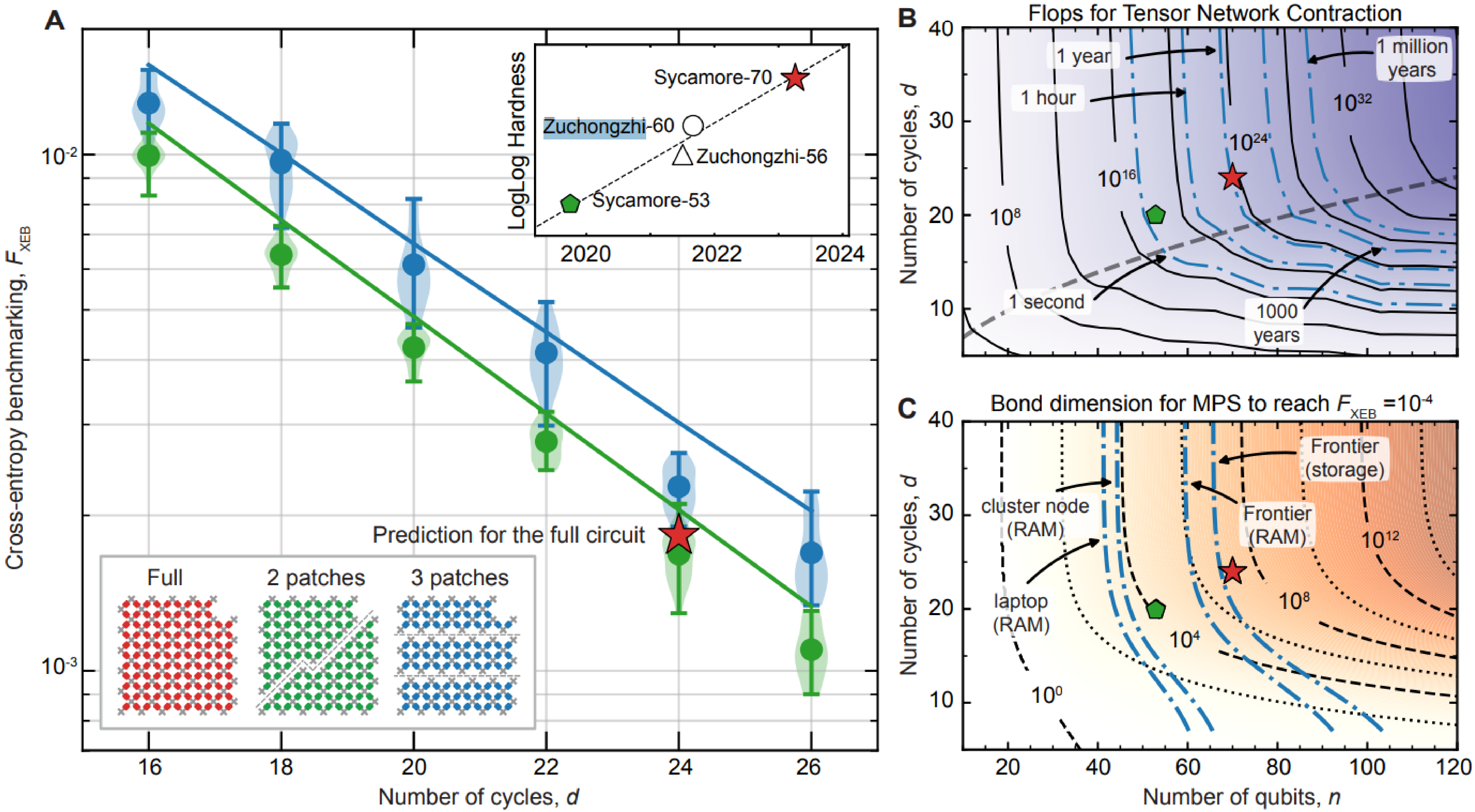

Quantum dynamics of T.F. Ising model

J. Zhang et.al., Nature **551**, 601 (2017).

- $\mathcal{H} = \sum_{i<j} J_{ij}\sigma_i^x \cdot \sigma_j^x + B_z \sum_i \sigma_i^z$
- Trapped-ion quantum computer (up to 53 qubits)
- $J_{ij} \propto J_0/|i-j|^{0.8}$

$$C_2 = \frac{1}{N^2}\sum_{i,j}\langle\sigma_i^x\sigma_j^x\rangle$$

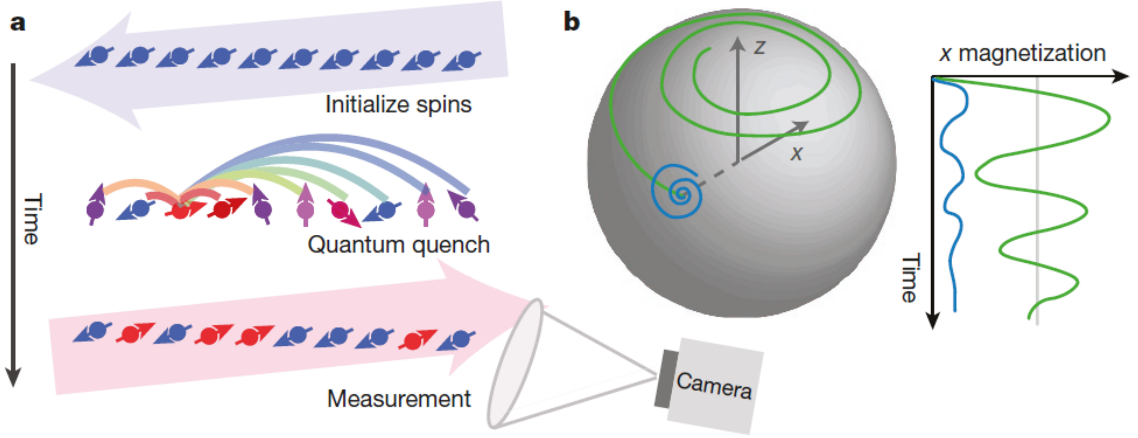

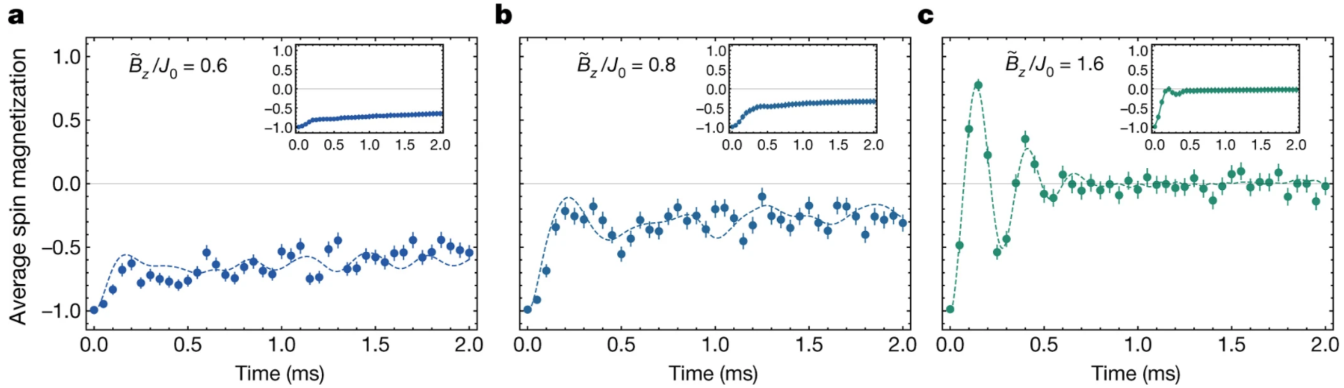

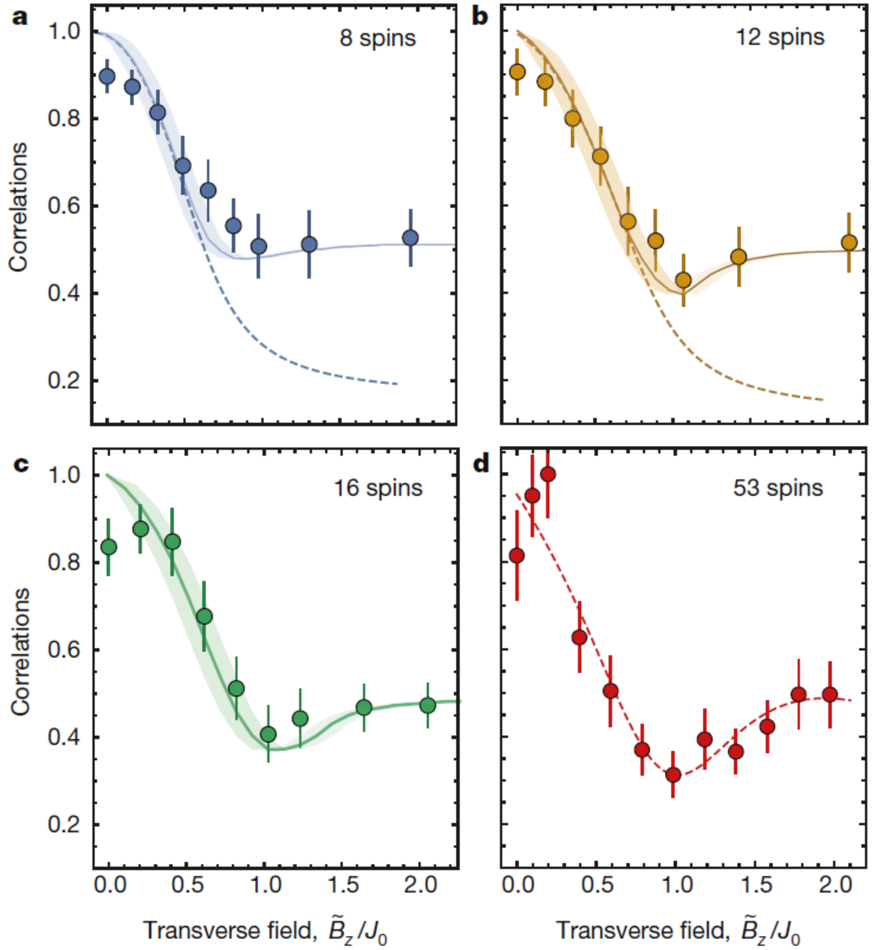

Quantum dynamics of T.F. Ising model

Y. Kim, et.al., Nature **618**, 500 (2023).

- Superconducting-type Q. device: 127 qubits

- Error mitigation processing is required.

  Probabilistic error cancellation (PEC)

  Zero-noise extrapolation (ZNE)

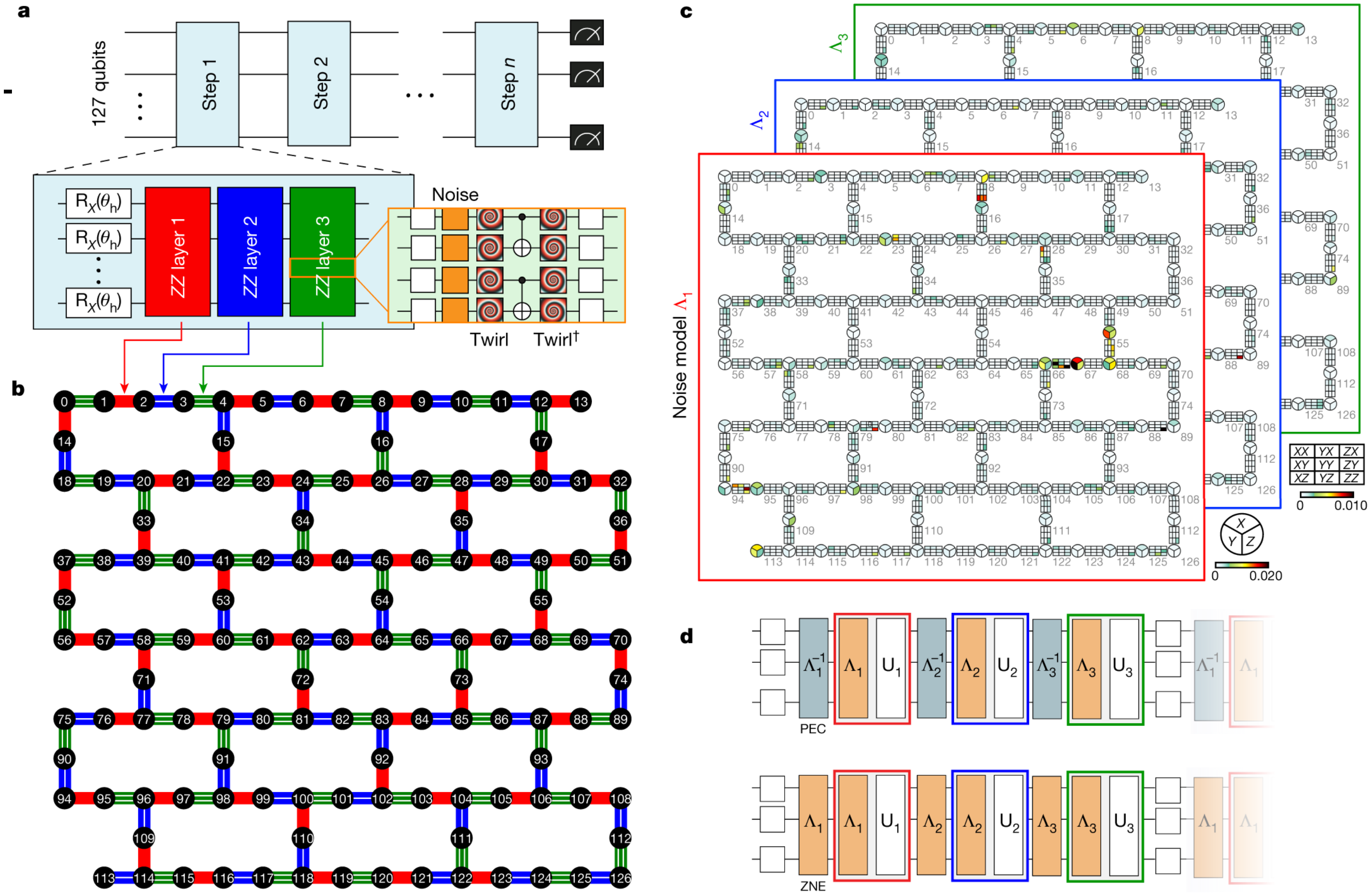

Quantum dynamics of T.F. Ising model

Y. Kim, et.al., Nature **618**, 500 (2023).

- # of Trotter steps： 5 (Computable with exact TN contraction of causal cones)
- Behavior not captured by TN methods (?)

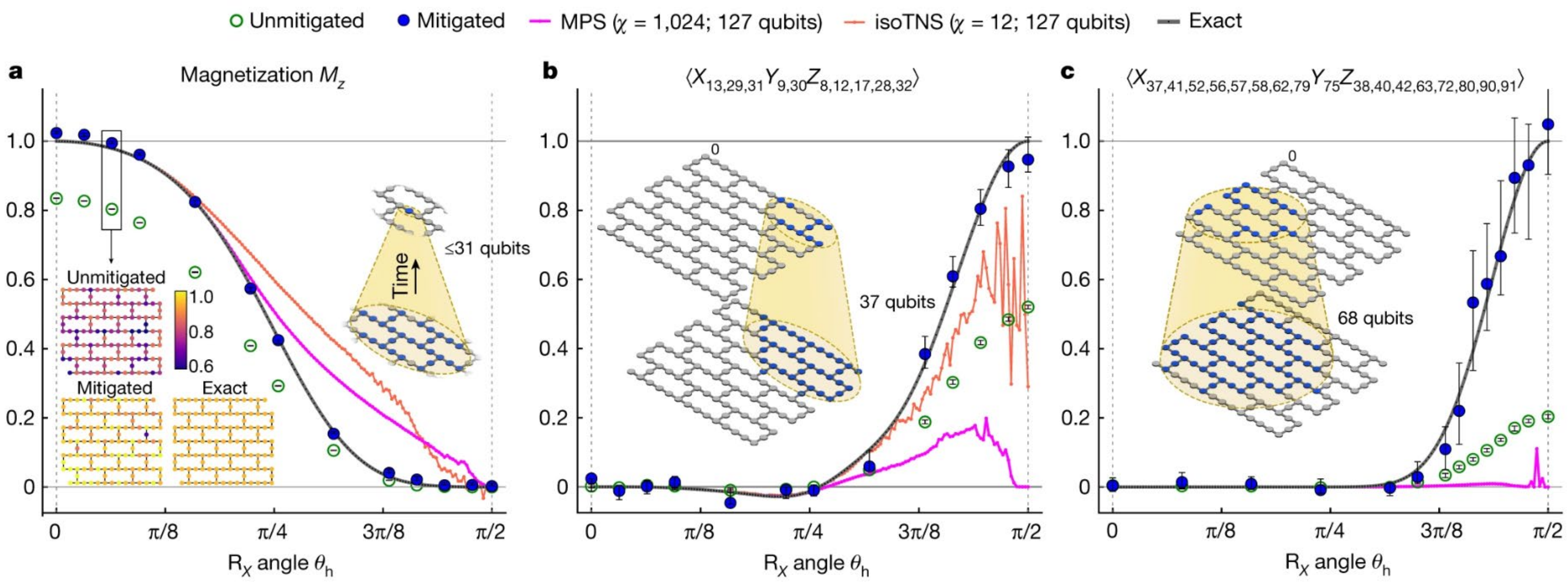

Reproduction by classical computations

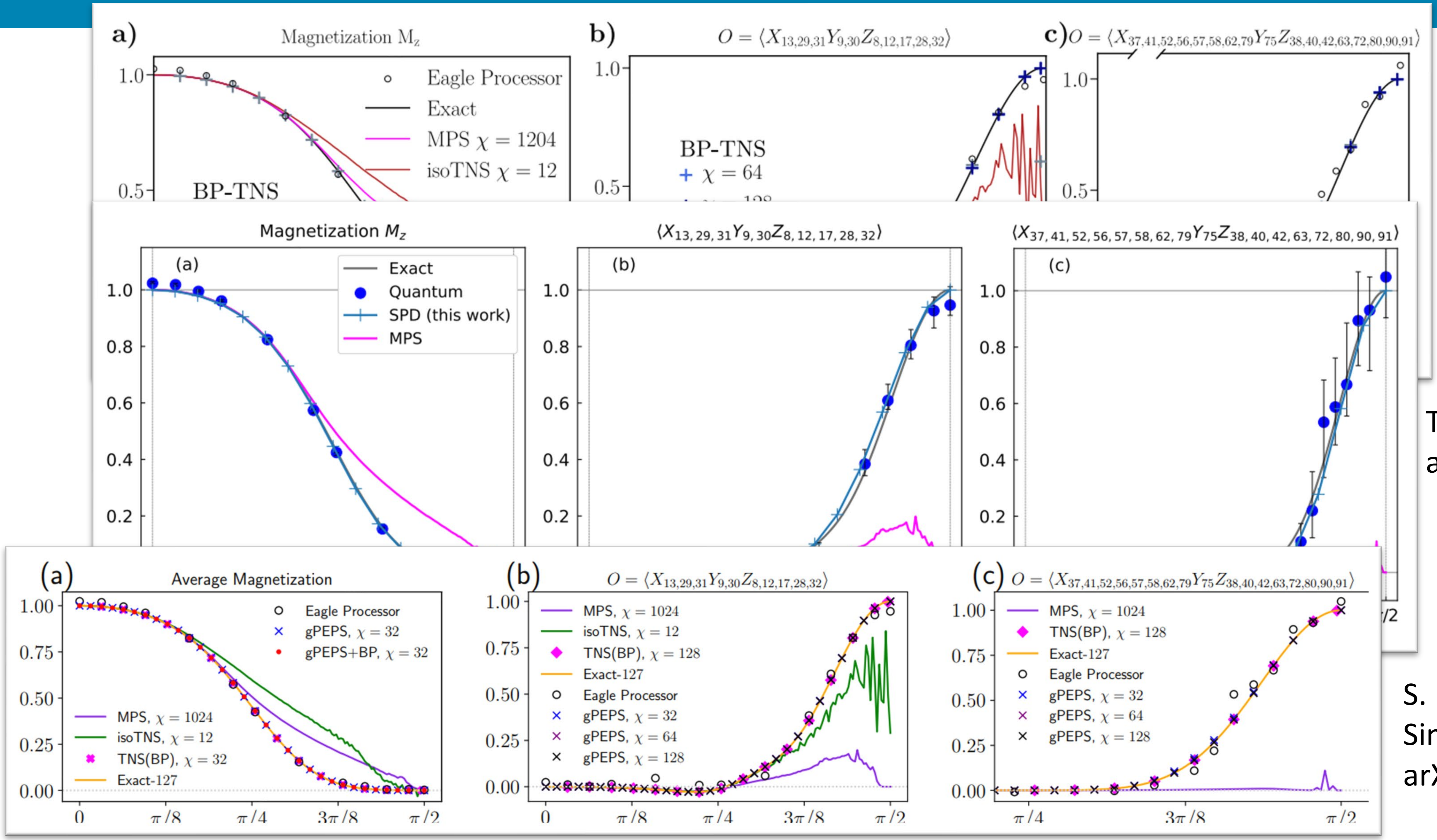

J. Tindall, M. Fishman, M. Stoudenmire, D. Sels, arXiv:2306.14887.

T. Begušić, G. K.-L. Chan, arXiv:2306.16372.

S. Patra, S. S. Jahromi, S. Singh, R. Orus, arXiv:2306.16372.

Calculations of G.S. for XXZ chains

H. Yu, et al., Phys. Rev. Res. **5**, 013183 (2023).

- $\mathcal{H} = \sum_{i=1}^{N-1}\left(\sigma_i^x\sigma_{i+1}^x + \sigma_i^y\sigma_{i+1}^y + \Delta\sigma_i^z\sigma_{i+1}^z\right)$
- Superconducting-type Q. device up to 102 qubits

magnetic model with uniaxial anisotropy

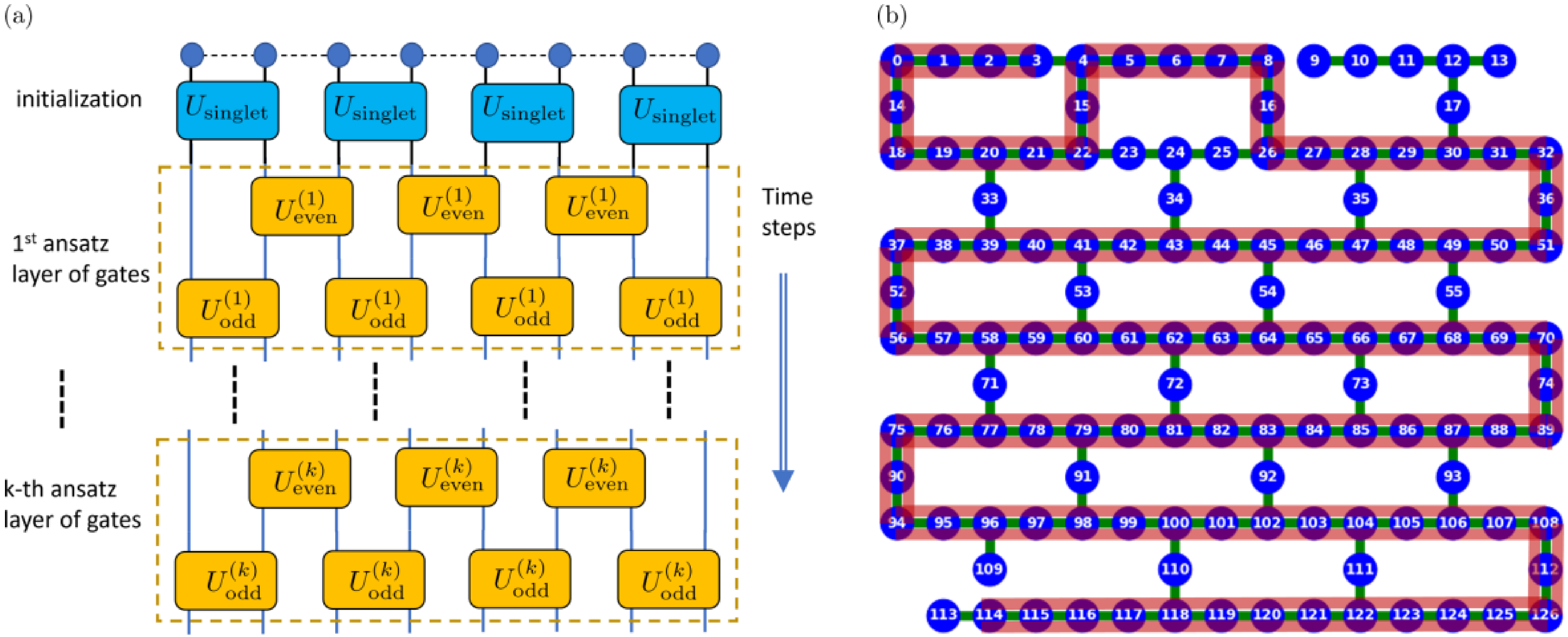

Calculations of G.S. for XXZ chains

H. Yu, et al., Phys. Rev. Res. **5**, 013183 (2023).

- $\mathcal{H} = \sum_{i=1}^{N-1}\left(\sigma_i^x\sigma_{i+1}^x + \sigma_i^y\sigma_{i+1}^y + \Delta\sigma_i^z\sigma_{i+1}^z\right)$
- Superconducting-type Q. device up to 102 qubits

magnetic model with uniaxial anisotropy

After error mitigation

N	θ^*_{even}	θ^*_{odd}	E^*_{ansatz}	E_{gs}	ϵ	f	E_{exp}	error
4	0.151748	0.215765	−6.464102	−6.464102	0	1.0000	−6.5(1.6)	0.56%
6	0.141671	0.216088	−9.880996	−9.974309	0.94%	0.9923	−9.9(1.9)*	0.19%
8	0.138569	0.216093	−13.299823	−13.499730	1.48%	0.9796	−13.2(2.2)	2.22%
10	0.13710	0.216102	−16.719307	−17.032141	1.84%	0.9639	−16.7(1.3)*	1.95%
12	0.136248	0.216110	−20.139037	−20.568363	2.09%	0.9462	−20.3(2.1)	1.30%
14	0.135688	0.216115	−23.558885	−24.106899	2.27%	0.9271	−23.6(1.8)	2.10%
16	0.135293	0.216120	−26.978800	−27.646949	2.42%	0.9072	−25.8(1.6)*	6.68%
18	0.134999	0.216123	−30.398756	−31.188044	2.53%	0.8867	−30.7(0.7)*	1.56%
20	0.134773	0.216126	−33.818738	−34.729893	2.62%	0.8659	−33.0(0.5)*	4.98%
30	0.134132	0.216134	−50.918850	−52.445423	2.91%	0.7614	−50.2(2.0)*	4.28%
40	0.133832	0.216139	−68.019098	−70.165893	3.06%	0.6629	−68.5(2.0)*	2.34%
50	0.133658	0.216141	−85.119397	−87.888441	3.15%	0.5737	−85.0(2.8)*	3.29%
60	0.133544	0.216143	−102.219721	−105.612060	3.21%	0.4946	−99(4)	6.26%
70	0.133464	0.216144	−119.320058	−123.336305	3.26%	0.4253	−125(7)	1.35%
80	0.133405	0.216145	−136.420403	−141.060947	3.29%	0.3649	−138.5(2.5)	1.82%
90	0.133359	0.216146	−153.520754	−158.785857	3.32%	0.3126	−153(5)	3.64%
98	0.133329	0.216146	−167.201038	−172.965924	3.33%	0.2760	−168.1(2.6)	2.81%
100	0.133323	0.216146	−170.621109	−176.510957	3.34%	0.2675	−173(9)	1.99%
102	0.133316	0.216146	−174.041180	−180.055995	3.34%	0.2592	−177.5(2.7)	1.42%

QS for quantum-many-body systems

Near-term algorithm

A. Peruzzo et al.
Nat. Commun (2014).

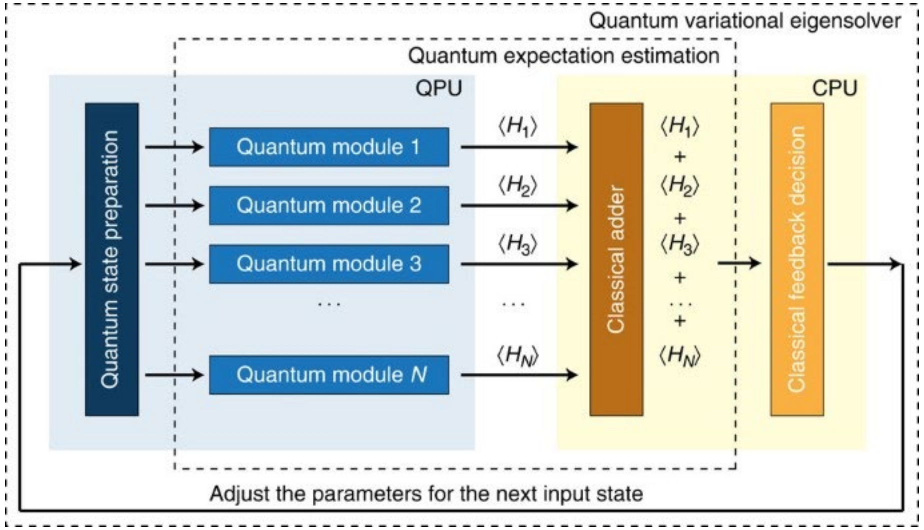

Variational quantum eigensolver (VQE)

Long-term algorithm

M. Nielsen and I. Chuang,
“Quantum Computation and
Quantum Information“

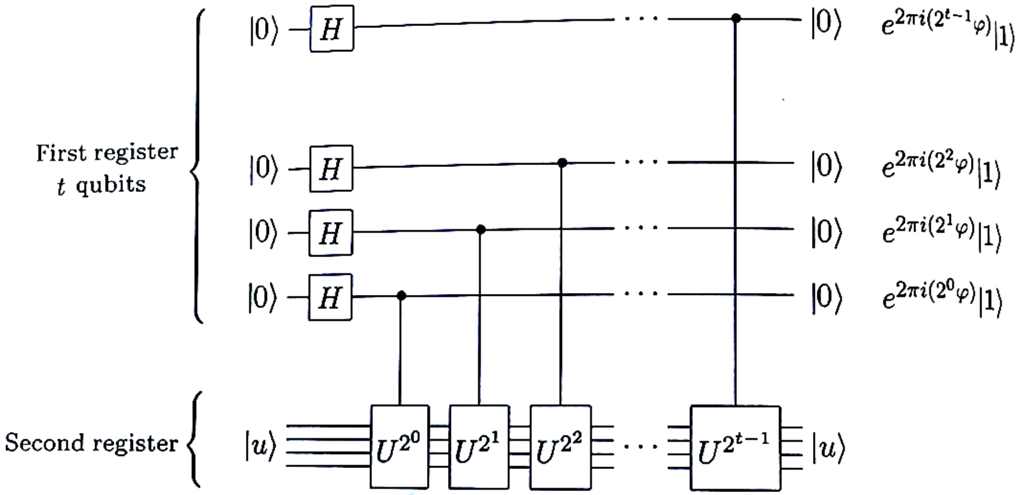

Quantum Phase estimation (QPE)

Common desirable condition: $\left| |\Psi_{\rm i}\rangle - |\Psi\rangle \right| < \epsilon$

Initial quantum state: $|\Psi_{\rm i}\rangle$, Target quantum (eigen)state: $|\Psi\rangle$

Key technique: Q Circuit Encoding (QCE)

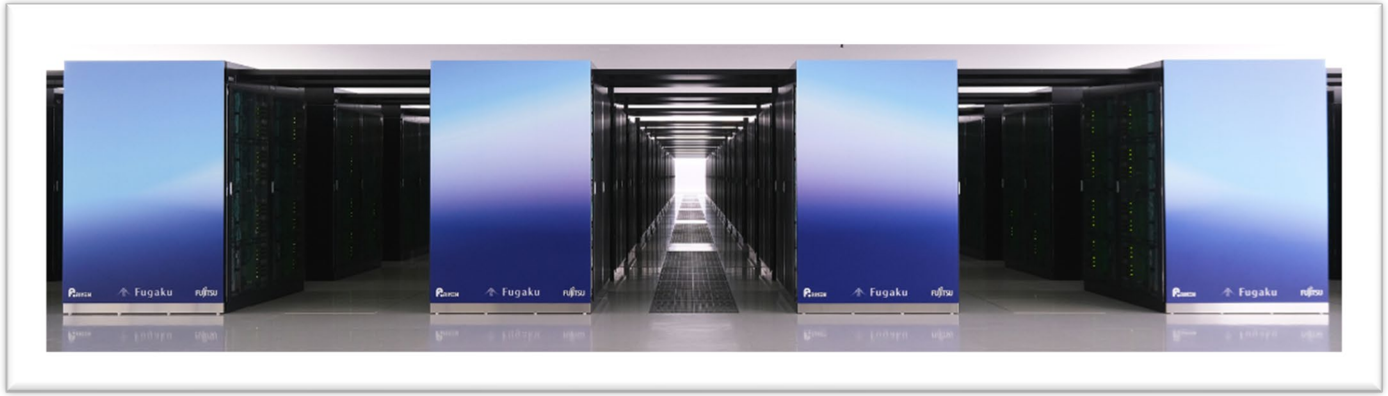

Classical computer

Quantum computer

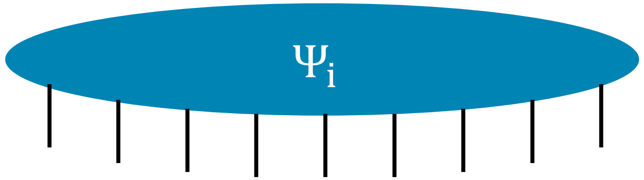

QCE

Amplitude Encoding

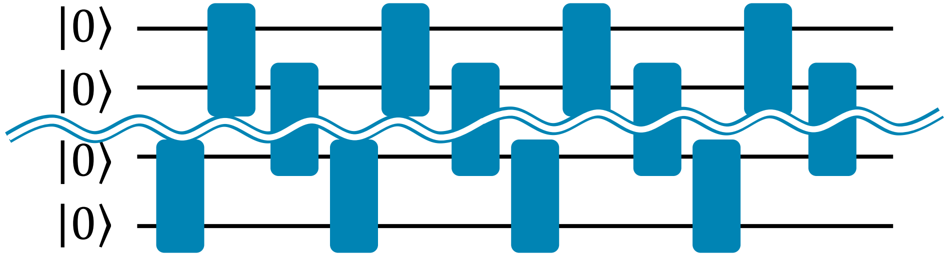

Exact encoding: Exponential circuit depth w/o ancillary qubits

Exponential # of ancillary qubits w/o exponential circuit depth

Powerful (approximate) QCE technique are demanded for QS !

Key idea: Tensor network decomposition

Review: R. Orus, Ann.Phys. **349**, 117 (2014).

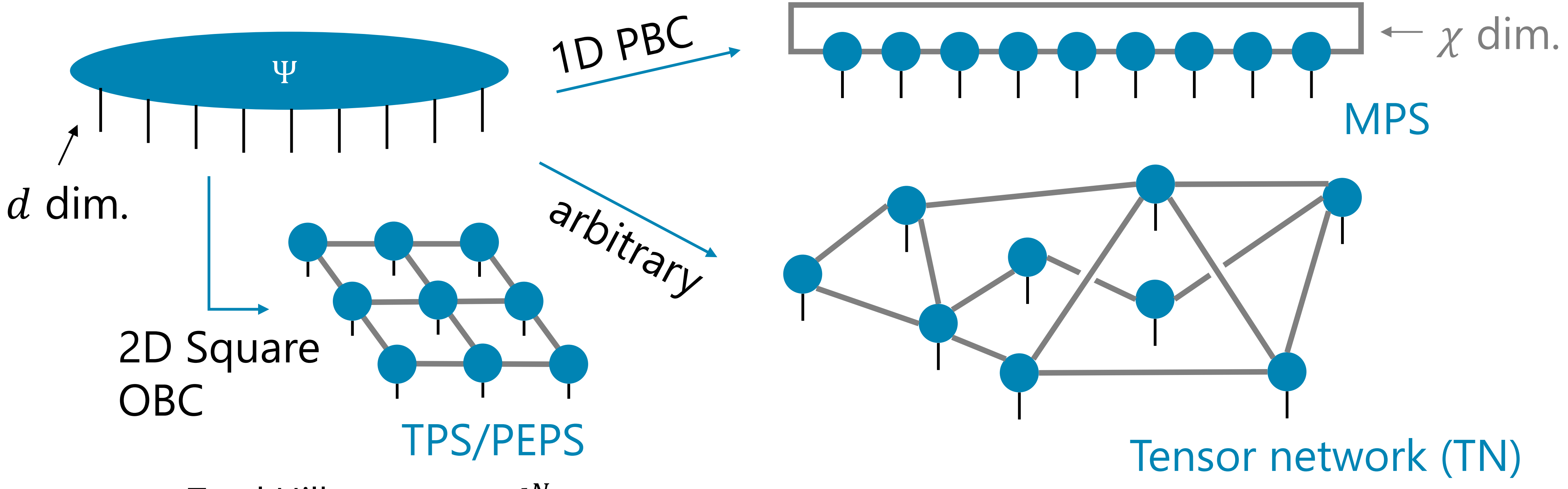

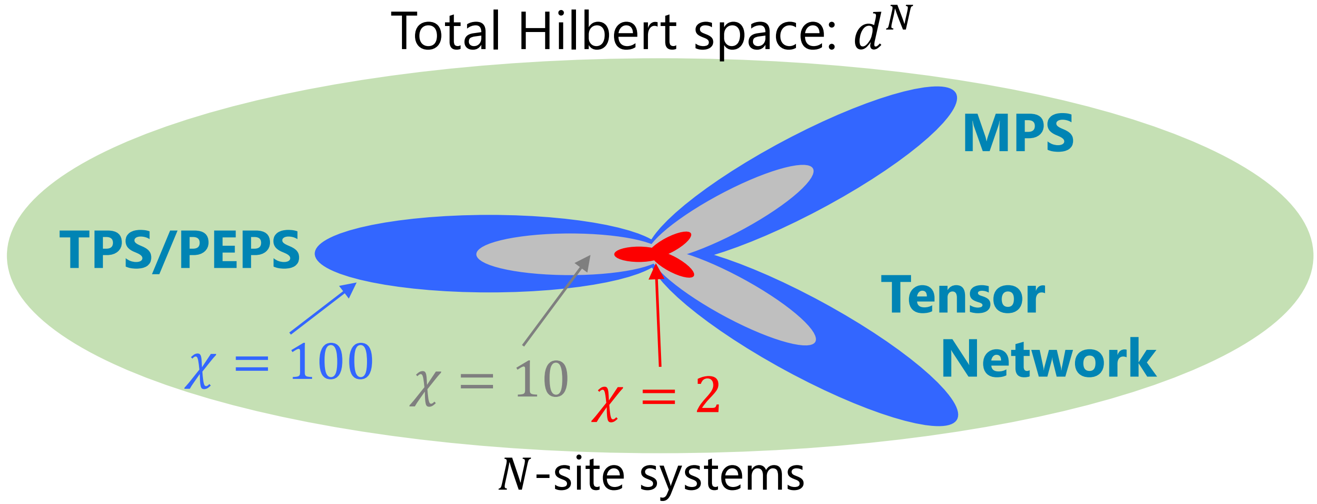

Good TN $\Leftrightarrow$ Good approximation of target quantum states with small χ

Contributed to the advancement of (approximate) QCE

最近携わったお仕事一覧

- TNの最適化原理を活用した自動量子回路エンコーディング

  T. Shirakawa, **<u>HU</u>**, S. Yunoki, arXiv: 2112.14524 (2021).

  - TTNの構造探索と最適化

    T. Hikihara, **<u>HU</u>**, K. Okunishi, K. Harada, T. Nishino, Phys. Rev. Res. **5**, 013031 (2023).
    K. Okunishi, **<u>HU</u>**, T. Nishino, PTEP **2023**, 023A02 (2023).

    西野さんの講演

    - MERAの構造探索

      R. Watanabe, **<u>HU</u>**, in preparation.

- TTN構造を使った分割統治VQE

  K. Fujii, K. Mizuta, **<u>HU</u>**, et al., PRX Quantum **3**, 010346 (2022).

- MERA/分岐MERAの構造を活用したTN&VQE相乗フレームワークの拡張

  R. Watanabe, K. Fujii, **HU**, arXiv:2305.06536 (2023).

- TNと直交関数展開を活用した量子状態振幅にエンコードされた関数の抽出

  K. Miyamoto, **<u>HU</u>**, Quantum Inf. Process. **22** 239 (2023).

- ダイヤモンド型量子回路による量子ダイナミクス計算

  S. Miyakoshi, T. Sugimoto, T. Shirakawa, S. Yunoki, **HU**, arxiv:2311.05900 (2023).

最近携わったお仕事一覧

- TNの最適化原理を活用した自動量子回路エンコーディング
  T. Shirakawa, **HU**, S. Yunoki, arXiv: 2112.14524 (2021).
  - TTNの構造探索と最適化
    T. Hikihara, **HU**, K. Okunishi, K. Harada, T. Nishino, Phys. Rev. Res. **5**, 013031 (2023).
    K. Okunishi, **HU**, T. Nishino, PTEP **2023**, 023A02 (2023).
    - MERAの構造探索
      R. Watanabe, **HU**, in preparation.

西野さんの講演

- TTN構造を使った分割統治VQE
  K. Fujii, K. Mizuta, **HU**, et al., PRX Quantum **3**, 010346 (2022).
- MERA/分岐MERAの構造を活用したTN&VQE相乗フレームワークの拡張
  R. Watanabe, K. Fujii, **HU**, arXiv:2305.06536 (2023).
- TNと直交関数展開を活用した量子状態振幅にエンコードされた関数の抽出
  K. Miyamoto, **HU**, Quantum Inf. Process. **22** 239 (2023).
- ダイヤモンド型量子回路による量子ダイナミクス計算
  S. Miyakoshi, T. Sugimoto, T. Shirakawa, S. Yunoki, **HU**, arxiv:2311.05900 (2023).

Set up of automatic QC encoder (AQCE)

- Given quantum states: $|\Psi\rangle = \sum_{\gamma=1}^{\Gamma} \chi_\gamma \hat{\psi}^{(\gamma)} |0\rangle$; complex value, QC/unitary ope.
- Fidelity: $F = \langle 0|\hat{\mathcal{U}}_1^\dagger \hat{\mathcal{U}}_2^\dagger \cdots \hat{\mathcal{U}}_M^\dagger |\Psi\rangle$; $\hat{\mathcal{U}}_m$: a quantum gate

In our work, we employ only SU(4) gate.

- Optimization: $\max_{\boldsymbol{u}} |F|$
- Fidelity tensor for the mth gate:

✓ $\hat{\mathcal{F}}_m = \mathrm{Tr}_{\bar{\mathbb{I}}_m}[|\Psi_{m+1}\rangle\langle\Phi_{m-1}|] =$ 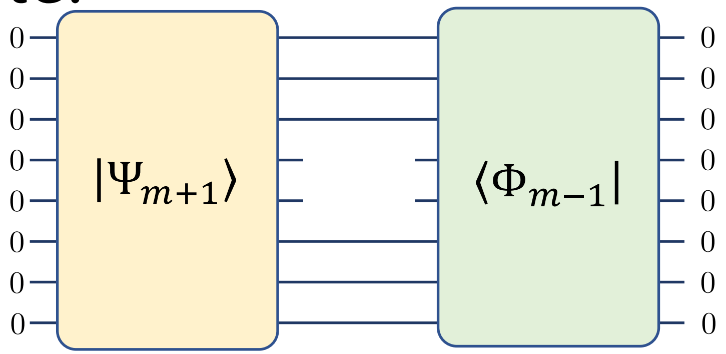

✓ $|\Psi_{m+1}\rangle = \hat{\mathcal{U}}_{m+1}^\dagger \cdots \hat{\mathcal{U}}_M^\dagger |\Psi\rangle$ and $\langle\Phi_{m-1}| = \langle 0|\hat{\mathcal{U}}_1^\dagger \cdots \hat{\mathcal{U}}_{m-1}^\dagger$

✓ $F = \mathrm{Tr}_{\mathbb{I}_m}\left[\hat{\mathcal{F}}_m \hat{\mathcal{U}}_m^\dagger\right] = \mathrm{tr}\left[\boldsymbol{F}_m \boldsymbol{U}_m^\dagger\right]$ ($\boldsymbol{F}_m$ and $\boldsymbol{U}_m^\dagger$ are 4-dim. mat.)

TN-inspired gradient-free optimization

- Key: Singular value decomposition (SVD)
  - ✓$\boldsymbol{F}_m \overset{\mathrm{svd}}{=} \boldsymbol{XDY}$; non-negative real diag. mat., unitary mat.
  - ✓$F = \mathrm{tr}\left[\boldsymbol{XDYU}_m^\dagger\right] = \sum_n [\boldsymbol{D}]_{nn} [\boldsymbol{Z}]_{nn}$
  - ✓$|F| = \left|\sum_n [\boldsymbol{D}]_{nn} [\boldsymbol{Z}]_{nn}\right| \leq \sum_n [\boldsymbol{D}]_{nn} \left|[\boldsymbol{Z}]_{nn}\right| \leq \sum_n [\boldsymbol{D}]_{nn}$

    the equalities hold if and only if $|[\boldsymbol{Z}]_{11}| = |[\boldsymbol{Z}]_{22}| = |[\boldsymbol{Z}]_{33}| = |[\boldsymbol{Z}]_{44}| = 1.$
  - ✓Maximization of $|F| \Leftrightarrow \boldsymbol{U}_m = \boldsymbol{XY}$
- Explicitly expand the linear combination
  - ✓$\hat{\mathcal{F}}_m = \sum_\gamma \chi_\gamma \mathrm{Tr}_{\bar{\mathbb{I}}_m}\left[\left|\psi_{m+1}^{(\gamma)}\right\rangle\langle\Phi_{m-1}|\right]$ with $\left|\psi_{m+1}^{(\gamma)}\right\rangle = \hat{\mathcal{U}}_{m+1}^\dagger \cdots \hat{\mathcal{U}}_M^\dagger \hat{\psi}^{(\gamma)}|0\rangle$

Assignment of quantum gates for SU(2) operator

- Euler rotation gate: $\hat{\mathcal{R}}(\boldsymbol{\theta}) = e^{-\mathrm{i}\theta_3\hat{Z}/2}e^{-\mathrm{i}\theta_2\hat{Y}/2}e^{-\mathrm{i}\theta_1\hat{Z}/2}$
- Mat. Rep.: $\boldsymbol{R} = \begin{pmatrix} e^{\mathrm{i}(\theta_3+\theta_1)/2}\cos(\theta_2/2) & -e^{\mathrm{i}(\theta_3-\theta_1)/2}\sin(\theta_2/2) \\ e^{\mathrm{i}(\theta_3-\theta_1)/2}\sin(\theta_2/2) & e^{\mathrm{i}(\theta_3+\theta_1)/2}\cos(\theta_2/2) \end{pmatrix}$
- Given rotation mat.: $\boldsymbol{V} = e^{-\mathrm{i}\theta_0/2}\boldsymbol{R}$

$\boldsymbol{m}$ determined to reproduce the sign of $\{v_{\sigma\sigma'}\}$

- Simultaneous nonlinear equations

$$\begin{aligned} v_{00} &= \mathrm{e}^{-\mathrm{i}(\theta_0+\theta_3+\theta_1)/2}\cos(\theta_2/2), \\ v_{10} &= \mathrm{e}^{-\mathrm{i}(\theta_0-\theta_3+\theta_1)/2}\sin(\theta_2/2), \\ v_{01} &= -\mathrm{e}^{-\mathrm{i}(\theta_0+\theta_3-\theta_1)/2}\sin(\theta_2/2), \\ v_{11} &= \mathrm{e}^{-\mathrm{i}(\theta_0-\theta_3-\theta_1)/2}\cos(\theta_2/2). \end{aligned}$$

$$\Rightarrow$$

$$\begin{aligned} \theta_0 &= \mathrm{i}\ln(v_{00}v_{11} - v_{10}v_{01}) + \pi m_0/2, \\ \theta_1 &= \mathrm{i}\ln\left(-\frac{v_{00}v_{10}}{v_{11}v_{01}}\right) + \pi m_1/2, \\ \theta_2 &= \arccos(\frac{1}{2}|v_{00}v_{11} + v_{10}v_{01}|) + \pi m_2/2, \\ \theta_3 &= \mathrm{i}\ln\left(-\frac{v_{00}v_{01}}{v_{11}v_{10}}\right) + \pi m_3/2 \end{aligned}$$

- In the special cases:

$v_{01} = v_{10} = 0$ & $v_{00}v_{11} \neq 0$

$$\begin{aligned} \theta_0 &= \mathrm{i}\ln(v_{00}v_{11}) + \pi m_0, \\ \theta_1 &= 2\mathrm{i}\ln\left(\frac{v_{00}}{v_{11}}\right) + \pi m_1, \\ \theta_2 &= 0, \\ \theta_3 &= 0. \end{aligned}$$

$v_{00} = v_{11} = 0$ & $v_{01}v_{10} \neq 0$

$$\begin{aligned} \theta_0 &= \mathrm{i}\ln(-v_{10}v_{01}) + \pi m_0, \\ \theta_1 &= \mathrm{i}\ln\left(-\frac{v_{10}}{v_{01}}\right) + \pi m_1, \\ \theta_2 &= \pi, \\ \theta_3 &= 0. \end{aligned}$$

Assignment of quantum gates for SU(4) operator

- Decomposition into a product of elementary gates

B. Kraus and J. I. Cirac, PRA 63, 062309 (2001).
G. Vidal and C. M. Dawson, PRA **69**, 010301 (2004).
Mark W. Coffey, et al., PRA **77**, 066301 (2008).

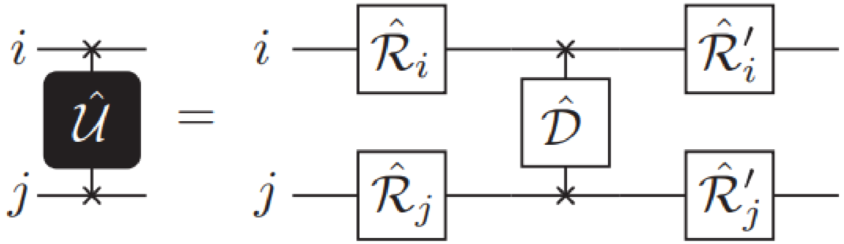

15 parameters
\+ global phase factor
($e^{i\alpha_0}$)

Consider $\hat{\mathcal{U}}$ in a magic (maximally entangled) basis set with

$$\hat{M} = \sum_{nk} |n\rangle\langle\phi_k| \doteq \frac{1}{\sqrt{2}}\begin{pmatrix} 1 & -i & 0 & 0 \\ 0 & 0 & -1 & -i \\ 0 & 0 & 1 & -i \\ 1 & i & 0 & 0 \end{pmatrix}$$

Good quantum numbers:
$\hat{X}_i\hat{X}_j|\phi_k\rangle = (-1)^{X_k}|\phi_k\rangle$
$[|\phi_k\rangle]^* = (-1)^{\Theta_k}|\phi_k\rangle$
$(X_k\Theta_k) \in \{(00), (11), (10), (01)\}$

$\hat{M}$ can be described by products of $\hat{H}$, $\hat{S}$ and CNOT gates

Euler rotation gates:

$$\hat{\mathcal{R}}_{q\in\{i,j\}} = e^{-i\xi_1^q \hat{Z}_q/2} e^{-i\xi_2^q \hat{Y}_q/2} e^{-i\xi_3^q \hat{Z}_q/2}$$

$$\hat{\mathcal{R}}'_{q\in\{i,j\}} = e^{-i\zeta_1^q \hat{Z}_q/2} e^{-i\zeta_2^q \hat{Y}_q/2} e^{-i\zeta_3^q \hat{Z}_q/2}$$

Canonical gates:

$$\hat{\mathcal{D}} = e^{-i(\alpha_1 \hat{X}_i \hat{X}_j + \alpha_2 \hat{Y}_i \hat{Y}_j + \alpha_3 \hat{Z}_i \hat{Z}_j)}$$

Hadamard & shift gates:

$$\hat{H} \doteq \frac{1}{\sqrt{2}}\begin{pmatrix} 1 & 1 \\ 1 & -1 \end{pmatrix}, \hat{S} = \begin{pmatrix} 1 & 0 \\ 0 & i \end{pmatrix}$$

Determination of $\hat{\mathcal{R}}_i, \hat{\mathcal{R}}_j, \hat{\mathcal{R}}'_i, \hat{\mathcal{R}}'_j$

Consider $\hat{\mathcal{U}}$ in a magic (maximally entangled) basis set $\{|\phi_k\rangle\}$

1. Unitary-symmetric mat.; $\hat{\mathcal{W}} = \hat{\mathcal{U}}^t\hat{\mathcal{U}}$;
2. Diagonalization: $\hat{\mathcal{W}} = \sum_k e^{2\mathrm{i}\varepsilon_k}|\psi_k\rangle\langle\psi_k|$,
   $|\psi_k\rangle = \sum'_k \mu_{kk'}|\phi_{k'}\rangle$ with orthonormal matrix $\boldsymbol{\mu}$
   maximally entangled!
3. Another maximally entangled basis set: $\{|\psi'_k\rangle = e^{-\mathrm{i}\varepsilon_k}\hat{\mathcal{U}}|\psi_k\rangle\}$
   $\hat{\mathcal{U}} = \sum_k e^{\mathrm{i}\varepsilon_k}|\psi'_k\rangle\langle\psi_k|$
4. A real in the magic basis: $|\bar{\psi}_k\rangle = e^{-\mathrm{i}\eta_k}|\psi_k\rangle$
5. Product states: $|\mu\rangle = (|\bar{\psi}_0\rangle + \mathrm{i}|\bar{\psi}_1\rangle)/\sqrt{2} = |a\rangle_i|b\rangle_j$, $|\nu\rangle = (|\bar{\psi}_0\rangle - \mathrm{i}|\bar{\psi}_1\rangle)/\sqrt{2} = |\bar{a}\rangle_i|\bar{b}\rangle_j$,
   in the same manner, $|\bar{\psi}_2\rangle = \left(e^{\mathrm{i}}|a\rangle_i|\bar{b}\rangle_j - e^{\mathrm{i}}|\bar{a}\rangle_i|b\rangle_j\right)/\sqrt{2}$, $|\bar{\psi}_3\rangle = \mathrm{i}\left(e^{\mathrm{i}\delta}|a\rangle_i|\bar{b}\rangle_j + e^{\mathrm{i}\delta}|\bar{a}\rangle_i|b\rangle_j\right)/\sqrt{2}$,
6. Euler rotation: $\hat{\mathcal{R}}_i = |0\rangle_i\langle a| + |1\rangle_i\langle\bar{a}|e^{\mathrm{i}\delta}, \hat{\mathcal{R}}_j = |0\rangle_j\langle b| + |1\rangle_j\langle\bar{b}|e^{-\mathrm{i}\delta}$
7. Get phase factor from MEMO III.
8. $\hat{\mathcal{R}}'_i$, $\hat{\mathcal{R}}'_j$ are determined through 4.-6. with $\{|\psi'_k\rangle\}$

MEMO:

I. $|\psi\rangle = \sum_k \mu_k|\phi_k\rangle$ is maximally entangled when $\mu_k \in \mathbb{R}$ for all k except for the global phase factor

II. Product state: $|a\rangle = \sum_k \mu_k|\phi_k\rangle$ with $\sum_k \mu_k^2 = 0$.

III. With certain local Euler rotations and phase factor: $|\phi_k\rangle = e^{\mathrm{i}\xi_k}\hat{\mathcal{R}}_i\hat{\mathcal{R}}_j|\psi_k\rangle$

Determination of $\widehat{\mathcal{D}}$ and Further decomposition

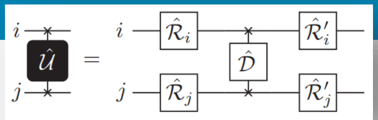

1. $$\hat{\mathcal{U}}|\psi_k\rangle = e^{i\varepsilon_k}|\psi'_k\rangle \rightarrow \underbrace{\hat{\mathcal{R}}'^{\dagger}_i \hat{\mathcal{R}}'^{\dagger}_j \hat{\mathcal{U}} \hat{\mathcal{R}}^{\dagger}_i \hat{\mathcal{R}}^{\dagger}_j}_{e^{-i\alpha_0}\widehat{\mathcal{D}}} |\phi_k\rangle = e^{-i(\xi'_k - \xi_k - \varepsilon_k)}|\phi_k\rangle$$
$$\rightarrow \alpha_0 + \lambda_k = \xi'_k - \xi_k - \varepsilon_k + 2\pi n_k$$

2. Using the relations:
$\widehat{\mathcal{D}}|\phi_k\rangle = e^{-i\lambda_k}|\phi_k\rangle$ with
$\lambda_0 = \alpha_1 - \alpha_2 + \alpha_3 + 2\pi n_0,$
$\lambda_1 = -\alpha_1 + \alpha_2 + \alpha_3 + 2\pi n_1,$
$\lambda_2 = -\alpha_1 - \alpha_2 - \alpha_3 + 2\pi n_2,$
$\lambda_3 = \alpha_1 + \alpha_2 - \alpha_3 + 2\pi n_3,$

We can determine
$\boldsymbol{\alpha} = (\alpha_1, \alpha_2, \alpha_3)$

3. 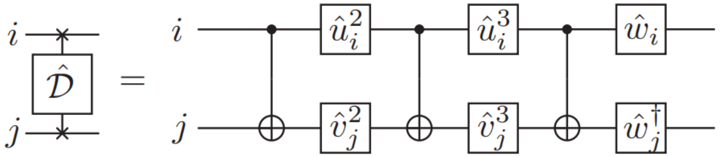

$$\hat{w}_i = e^{i\pi \hat{X}_i/4}, \quad \hat{w}_j^\dagger = e^{-i\pi \hat{X}_j/4},$$
$$\hat{u}_i^3 = \hat{H}_i \hat{S}_i, \quad \hat{v}_j^3 = e^{-i\alpha_2 \hat{Z}_j},$$
$$\hat{u}_i^2 = \hat{H}_i e^{i\alpha_1 \hat{X}_i}, \quad \hat{v}_j^2 = e^{i\alpha_3 \hat{Z}_j}$$

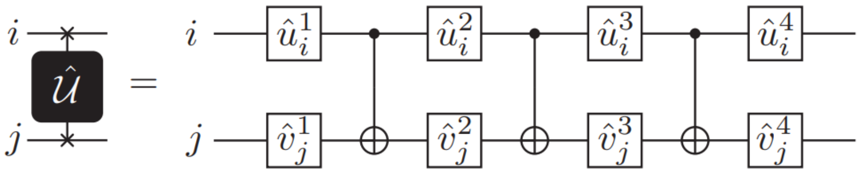

$$\hat{u}_i^1 = \hat{\mathcal{R}}_i, \quad \hat{v}_j^1 = \hat{\mathcal{R}}_j,$$
$$\hat{u}_i^4 = \hat{\mathcal{R}}'_i \hat{w}_i, \quad \hat{v}_j^4 = \hat{\mathcal{R}}'_j \hat{w}_j^\dagger.$$

Assigned algebraically !

MEMO:

I. $|\psi\rangle = \sum_k \mu_k |\phi_k\rangle$ is maximally entangled when $\mu_k \in \mathbb{R}$ for all k except for the global phase factor

II. Product state: $|a\rangle = \sum_k \mu_k |\phi_k\rangle$ with $\sum_k \mu_k^2 = 0.$

III. With certain local Euler rotations and phase factor: $|\phi_k\rangle = e^{i\xi_k} \hat{\mathcal{R}}_i \hat{\mathcal{R}}_j |\psi_k\rangle$

Quantum circuit encoding algorithm

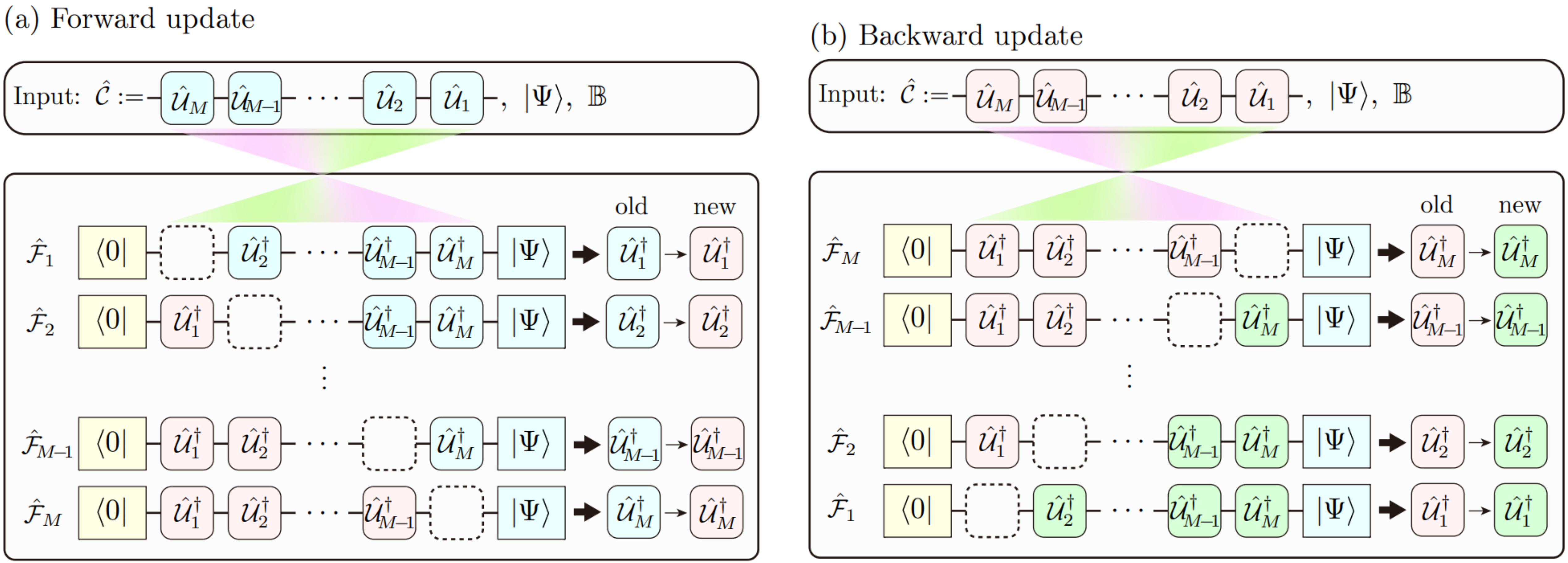

An optimal pair of bond $(i, j) \in \mathbb{B}$ is searched in each optimizations.
(A tensor network relaxation method)

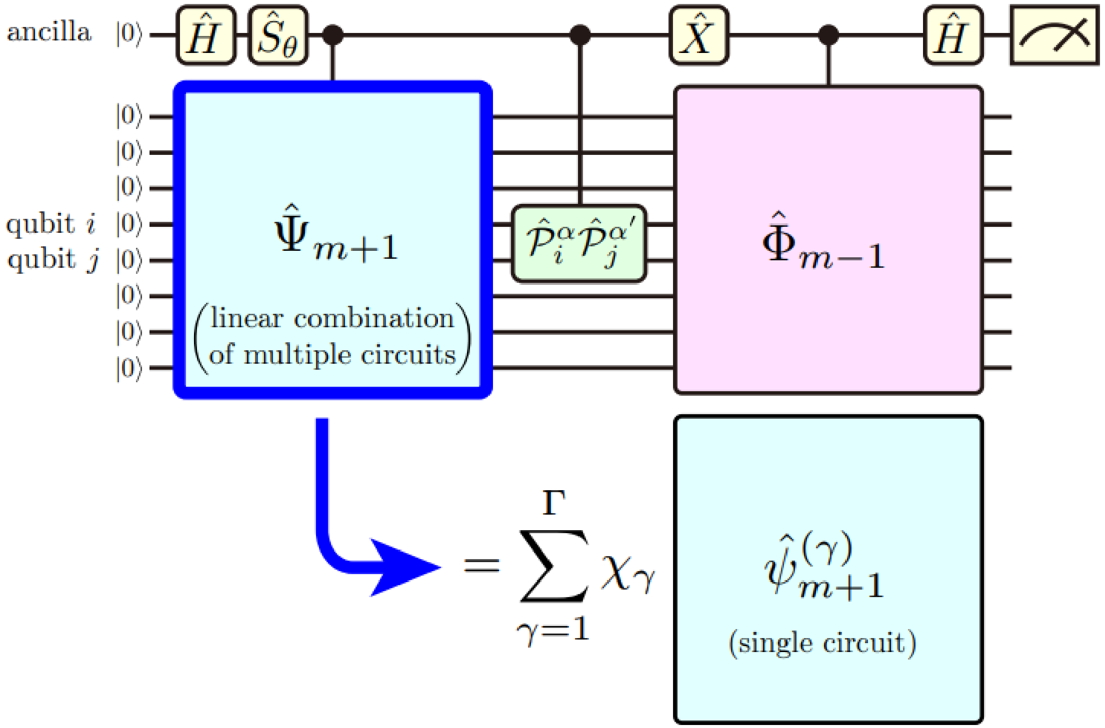

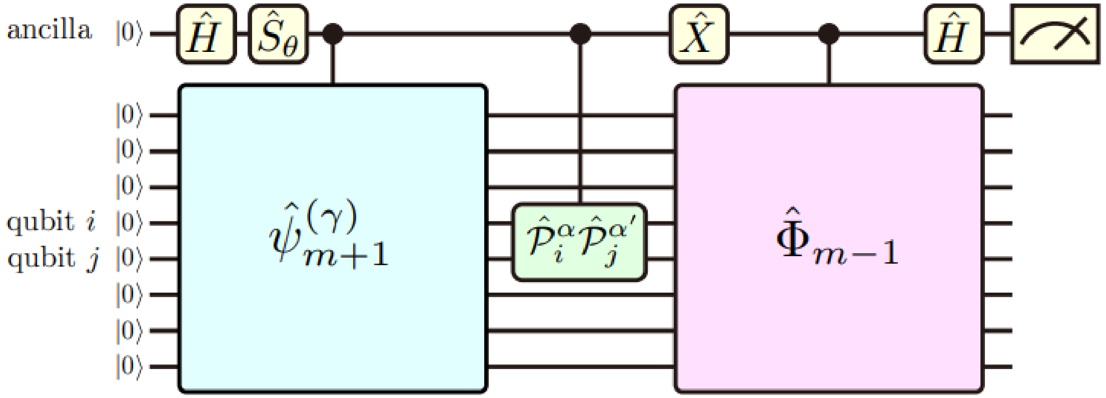

$$\hat{S}_\theta \doteq \begin{pmatrix} 1 & 0 \\ 0 & e^{-\mathrm{i}\theta} \end{pmatrix}, \ \hat{\mathcal{P}}_i^\alpha = \begin{cases} \hat{I}_i \ (\alpha = 0) \\ \hat{X}_i \ (\alpha = 1) \\ \hat{Y}_i \ (\alpha = 2) \\ \hat{Z}_i \ (\alpha = 3) \end{cases}$$

$$\hat{\mathcal{F}}_m = \mathrm{Tr}_{\bar{\mathbb{I}}_m}[|\Psi_{m+1}\rangle\langle\Phi_{m-1}|] = \sum_{\alpha\alpha'} \tilde{f}_{\alpha\alpha'} \hat{\mathcal{P}}_i^\alpha \hat{\mathcal{P}}_j^{\alpha'}$$

$$\mathrm{Tr}_{\mathbb{I}_m}\left[\hat{\mathcal{F}}_m \hat{\mathcal{P}}_i^\alpha \hat{\mathcal{P}}_j^{\alpha'}\right] = \langle\Phi_{m-1}|\hat{\mathcal{P}}_i^\alpha \hat{\mathcal{P}}_j^{\alpha'}|\Psi_{m+1}\rangle = 2^2 \tilde{f}_{\alpha\alpha'}$$

Explicitly expand the linear combination

$$\hat{\mathcal{F}}_m = \mathrm{Tr}_{\bar{\mathbb{I}}_m}[|\Psi_{m+1}\rangle\langle\Phi_{m-1}|] = \sum_{\alpha\alpha'} \tilde{f}_{\alpha\alpha'} \hat{\mathcal{P}}_i^\alpha \hat{\mathcal{P}}_j^{\alpha'}$$

$$\mathrm{Tr}_{\mathbb{I}_m}\left[\hat{\mathcal{F}}_m \hat{\mathcal{P}}_i^\alpha \hat{\mathcal{P}}_j^{\alpha'}\right] = \sum_{\gamma=1}^{\Gamma} \chi_\gamma \left\langle \Phi_{m-1} \middle| \hat{\mathcal{P}}_i^\alpha \hat{\mathcal{P}}_j^{\alpha'} \middle| \psi_{m+1}^{(\gamma)} \right\rangle$$
$$= 2^2 \sum_{\gamma=1}^{\Gamma} \chi_\gamma \tilde{f}_{\alpha\alpha'}^{(\gamma)}$$

Initialization algorithm

1. $|\varphi_0\rangle \coloneqq |\Psi\rangle$ and $m = 0$
2. Reduced density matrix: $\hat{\rho} \coloneqq \mathrm{Tr}_{\mathbb{I}_{m+1}}[|\varphi_m\rangle\langle\varphi_m|] = \sum_{nn'} \rho_{nn'}|n\rangle\langle n'|$
   $= \sum_{\alpha\alpha'} \tilde{r}_{\alpha\alpha'} \hat{\mathcal{P}}_i^{\alpha} \hat{\mathcal{P}}_j^{\alpha'}$
3. Diagonalization: $\hat{\rho} = \sum_n \lambda_n |\lambda_n\rangle\langle\lambda_n|$
4. Set init. circuit: $\hat{\mathcal{V}}_{m+1} = \sum_n |\lambda_n\rangle\langle n| = \arg\max\langle 0|\hat{\mathcal{V}}_{m+1}^{\dagger}\rho\hat{\mathcal{V}}_{m+1}|0\rangle$
5. Update: $|\varphi_{m+1}\rangle = \hat{\mathcal{V}}_{m+1}^{\dagger}|\varphi_m\rangle$
6. $m := m + 1$ and go to step 2 up to $m = \delta M$.

An optimal pair of bond $(i, j) \in \mathbb{B}$ is searched in each optimizations.
(A tensor network relaxation method)

Automatic quantum circuit encoding algorithm

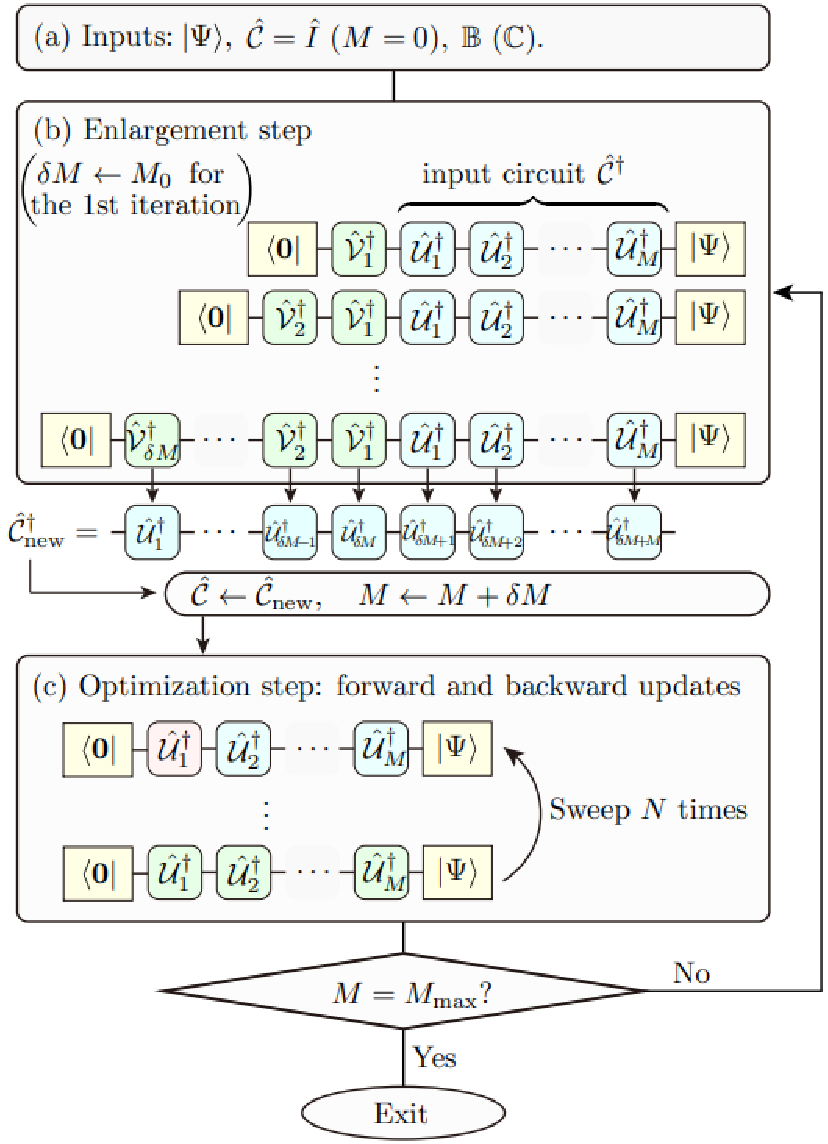

- Inputs:
  - ✓Target quantum state $|\Psi\rangle$
  - ✓Quantum circuit $\hat{\mathcal{C}} := \hat{I}$
  - ✓Set of bonds $\mathbb{B}$ of two qubits (or a set of clusters $\mathbb{C}$ of K qubits)
- Controlling parameters
  - ✓# of iterations for each Enlargement: δM
  - ✓Initial δM: M_0
  - ✓# of all quantum gates: M_{max}
  - ✓# of sweeps for each optimization: N

AQCE of quantum many-body states

- XXZ model: $\hat{\mathcal{H}} = \sum_{i=1}^{L} \hat{X}_i \hat{X}_{i+1} + \hat{Y}_i \hat{Y}_{i+1} + \Delta \hat{Z}_i \hat{Z}_{i+1}$
  - ✓Periodic boundary condition: $\hat{A}_{L+1} = \hat{A}_1; A \in \{X, Y, Z\}$
  - ✓$\Delta = 0$ (XY model), $\Delta = 1$ (Heisenberg model) : critical phase (the correlation length diverges)
  - ✓$|\Psi\rangle$ given by Lanczos method [accuracy of the G.S. energy 10^{-12}]
- Set up of AQCE
  - ✓100 different calculations (The result of AQCE is depends on the init. $|\Psi\rangle$)
  - ✓In the case of $\Delta = 0$: $(M_0, N, \delta M, M_{\max}) = (L, 20, L/2, L(L-5)/2)$
  - ✓ $\Delta = 1$: $(M_0, N, \delta M, M_{\max}) = (L, 20, L/2, L^2/2)$
  - ✓ $\mathbb{B}$ is composed of all pairs of two sites.

Monotonic decreasing of Fidelity error

$\Delta = 0$ (XY model)

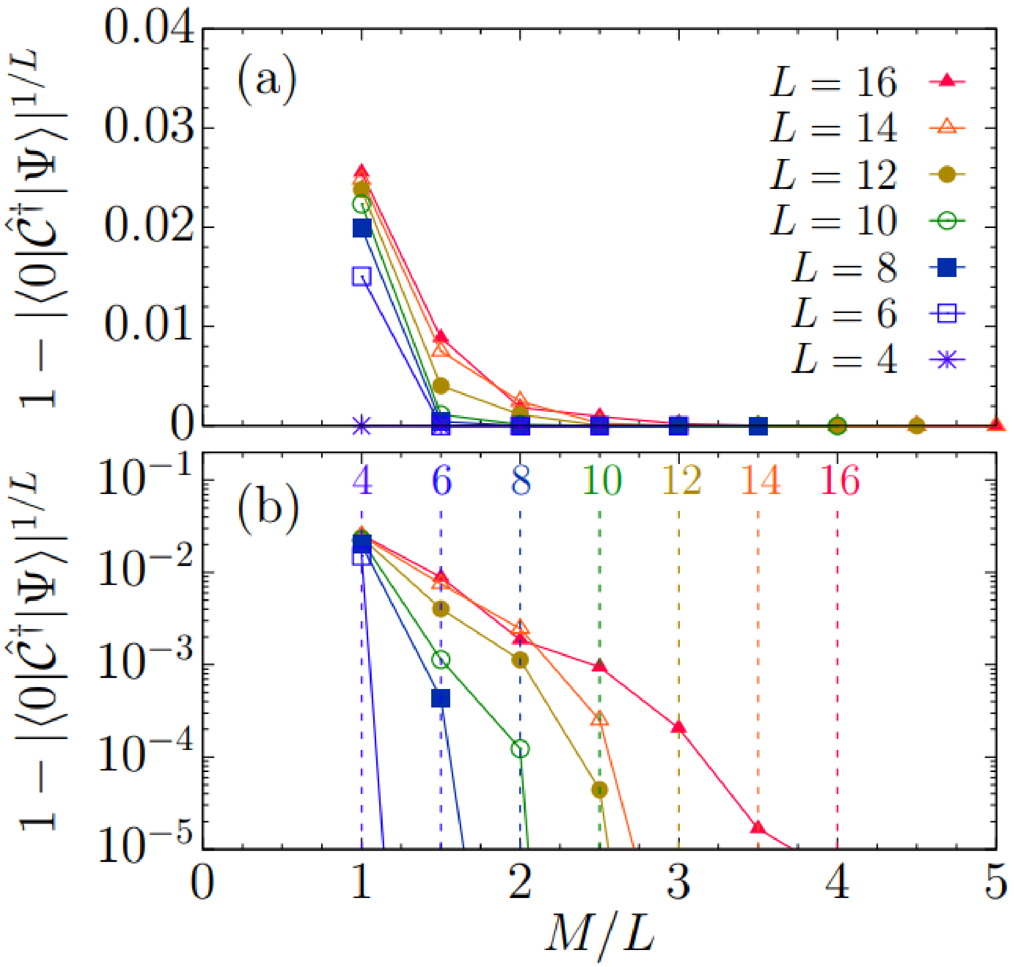

$\Delta = 1$ (Heisenberg model)

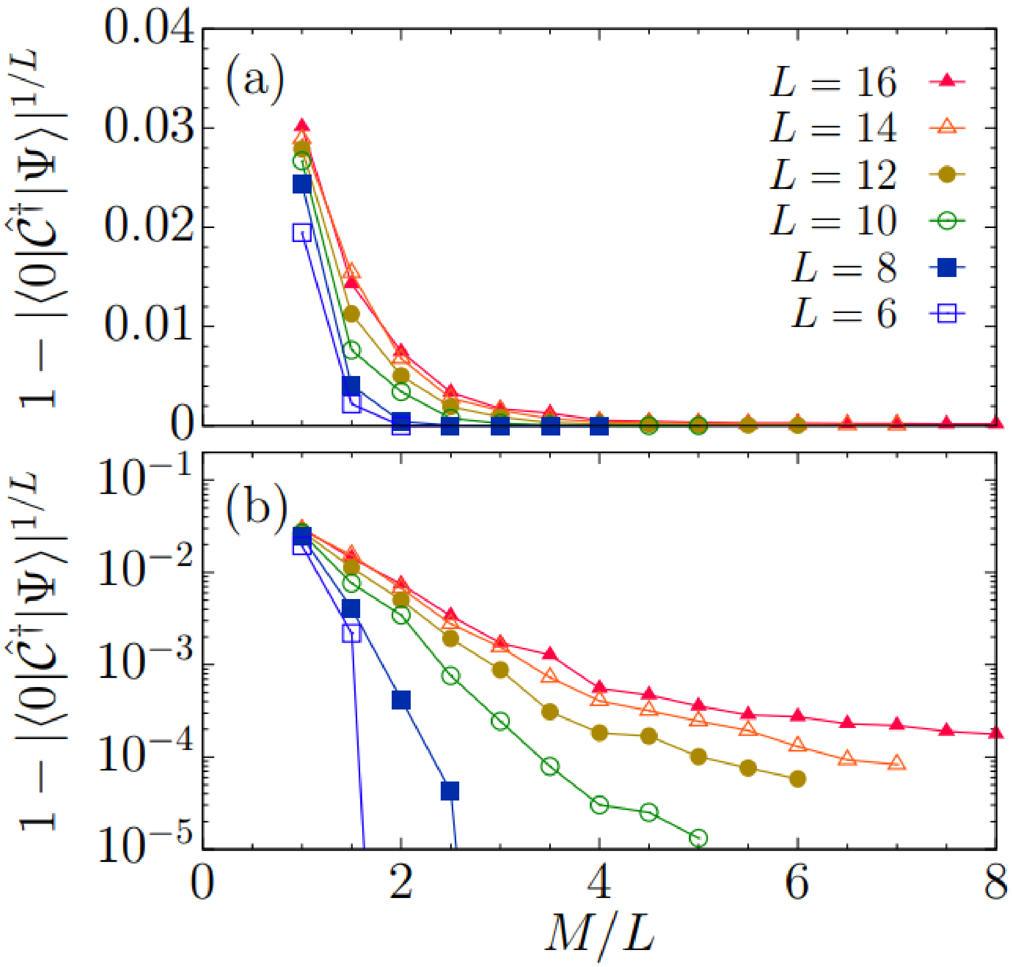

Monotonic decreasing of Fidelity error

$\Delta = 0$ (XY model)

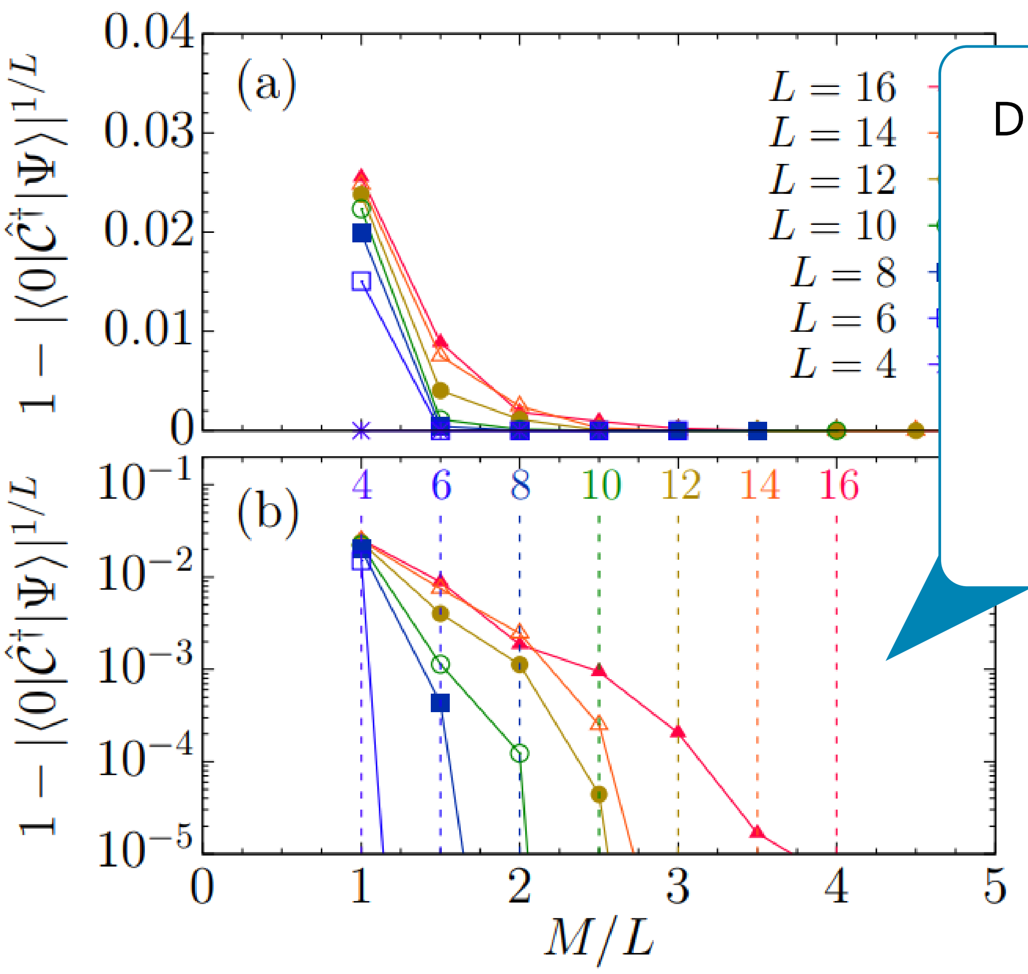

$\Delta = 1$ (Heisenberg model)

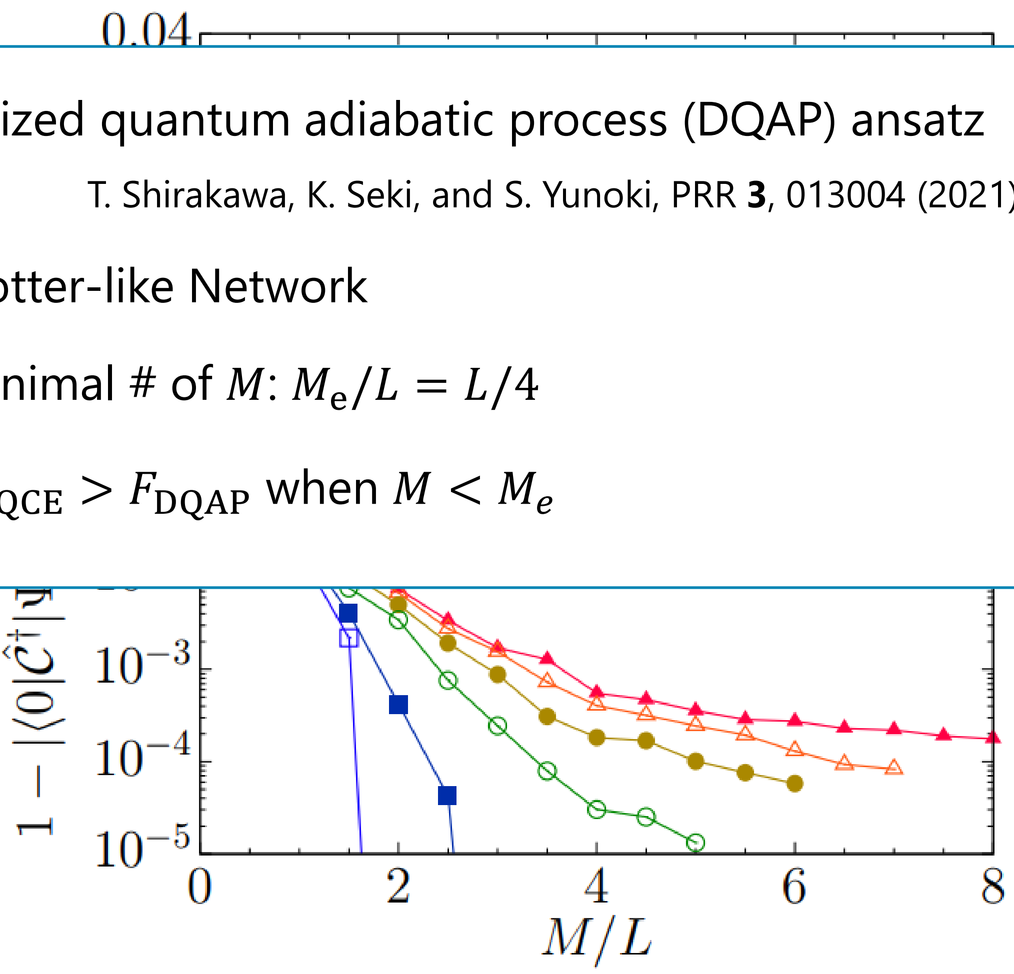

Discretized quantum adiabatic process (DQAP) ansatz

T. Shirakawa, K. Seki, and S. Yunoki, PRR **3**, 013004 (2021).

Trotter-like Network

Minimal # of M: $M_\mathrm{e}/L = L/4$

$F_\mathrm{AQCE} > F_\mathrm{DQAP}$ when $M < M_e$

Monotonic decreasing of Fidelity error

Non-uniform QC for Uniform G.S.

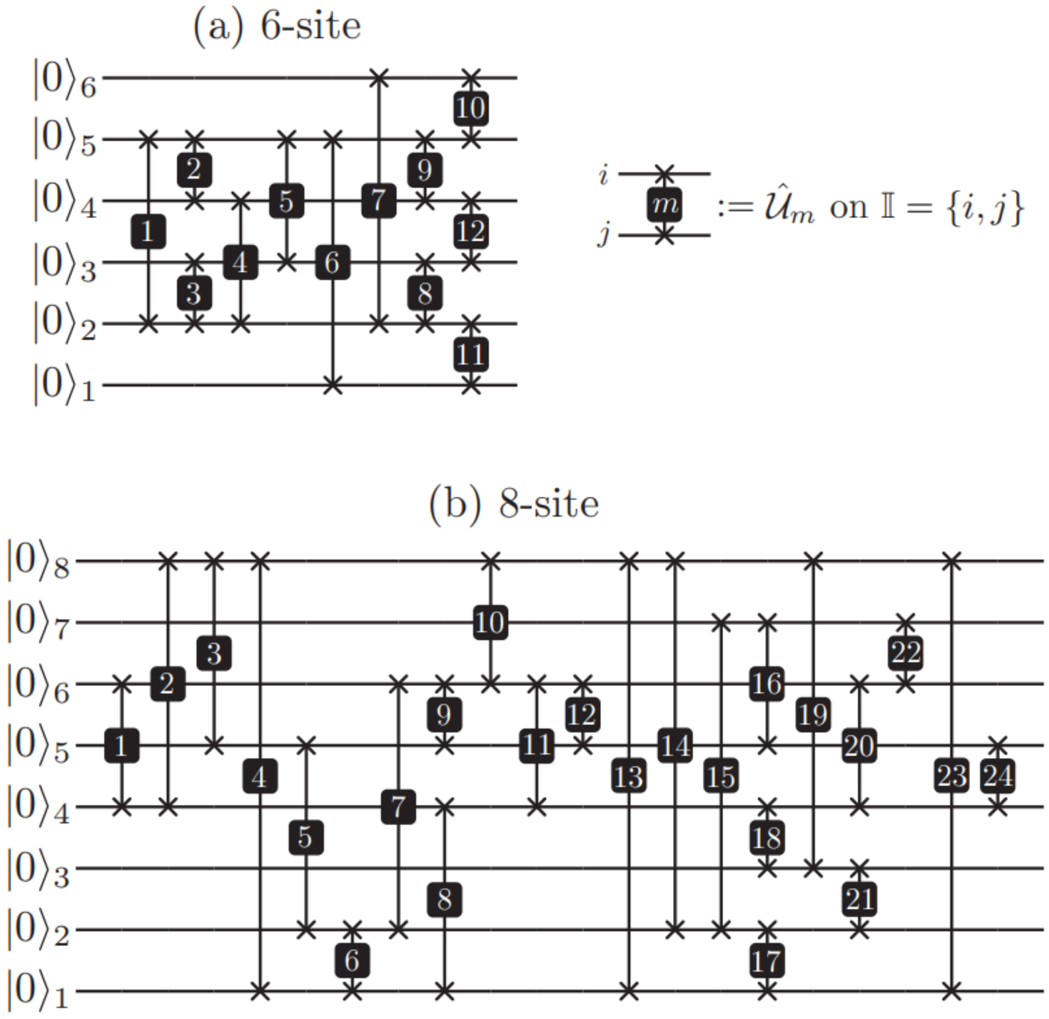

$\Delta = 1$ (Heisenberg model)

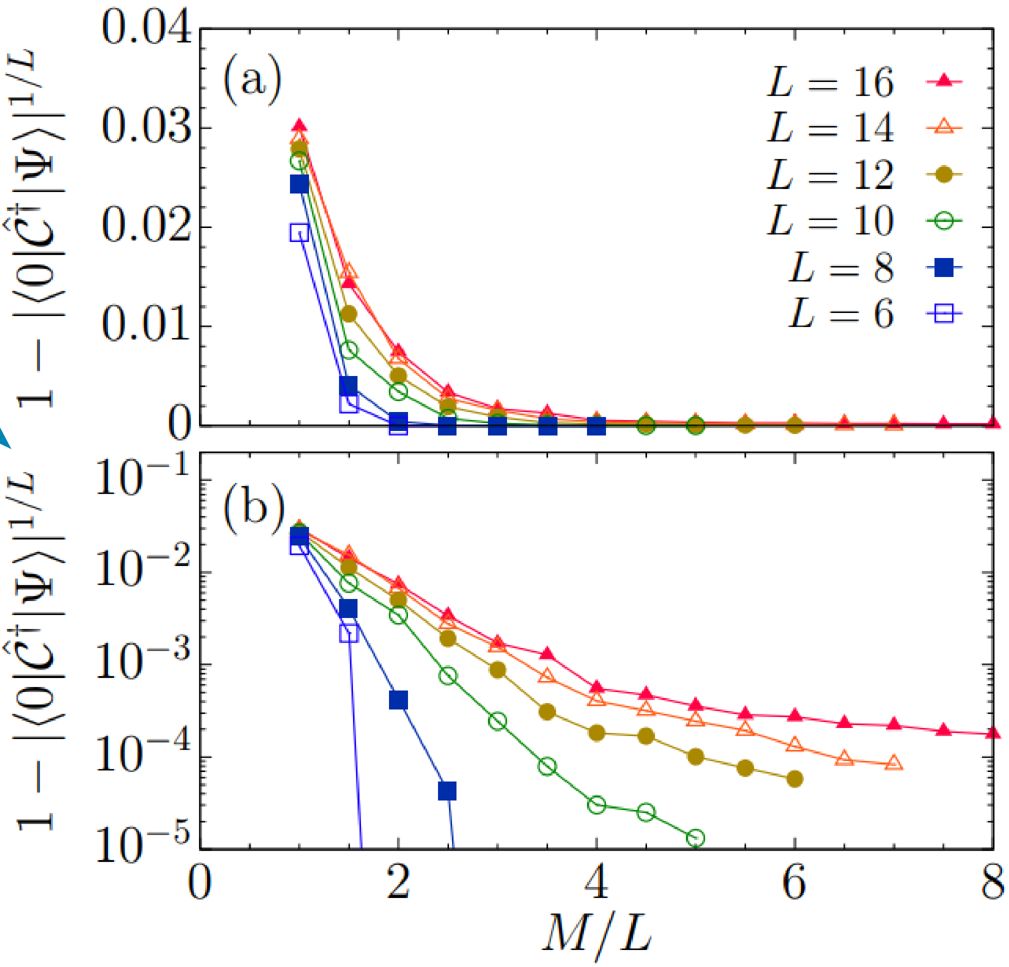

QCE with Fixed Trotter/MERA-like Net.

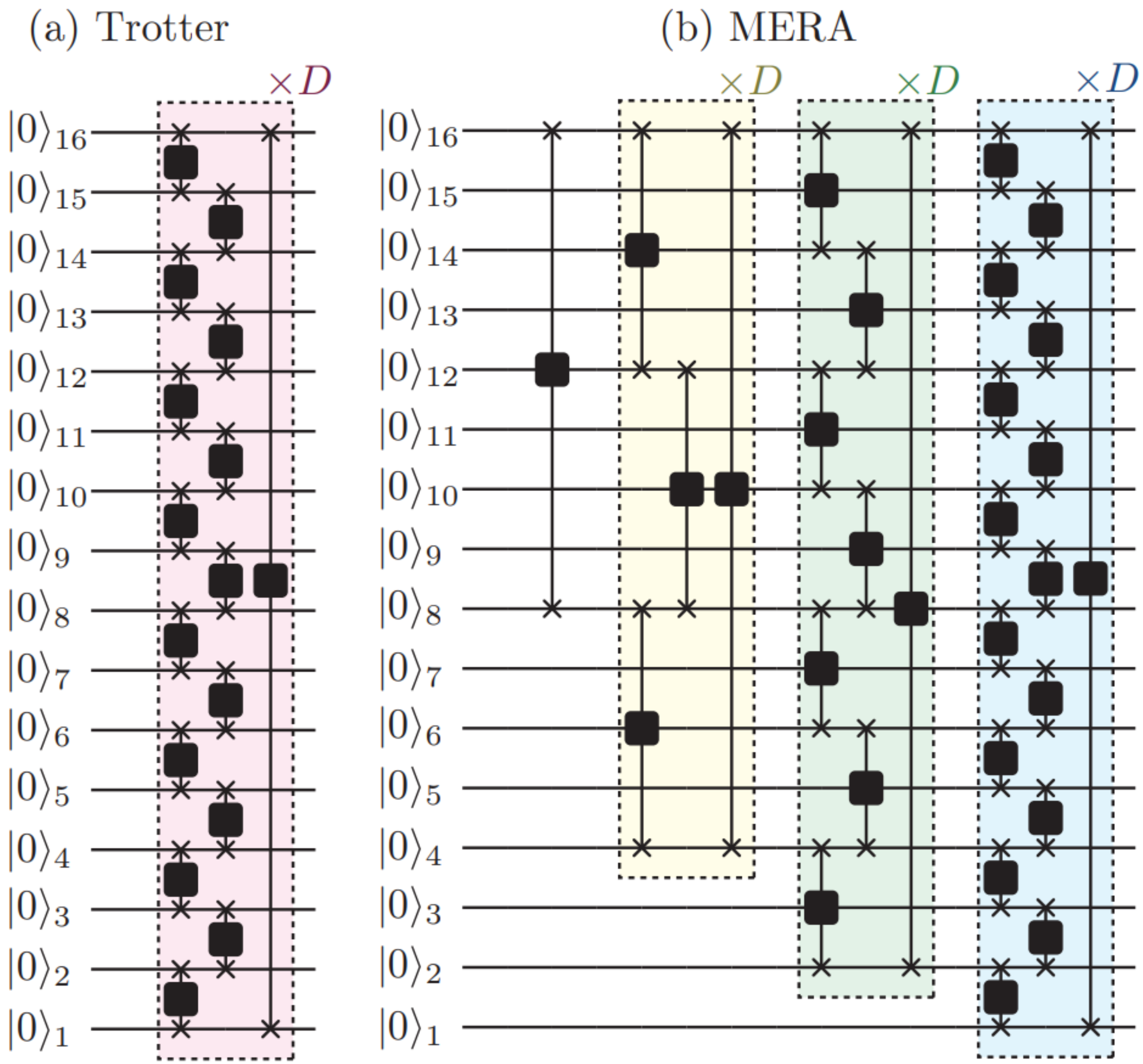

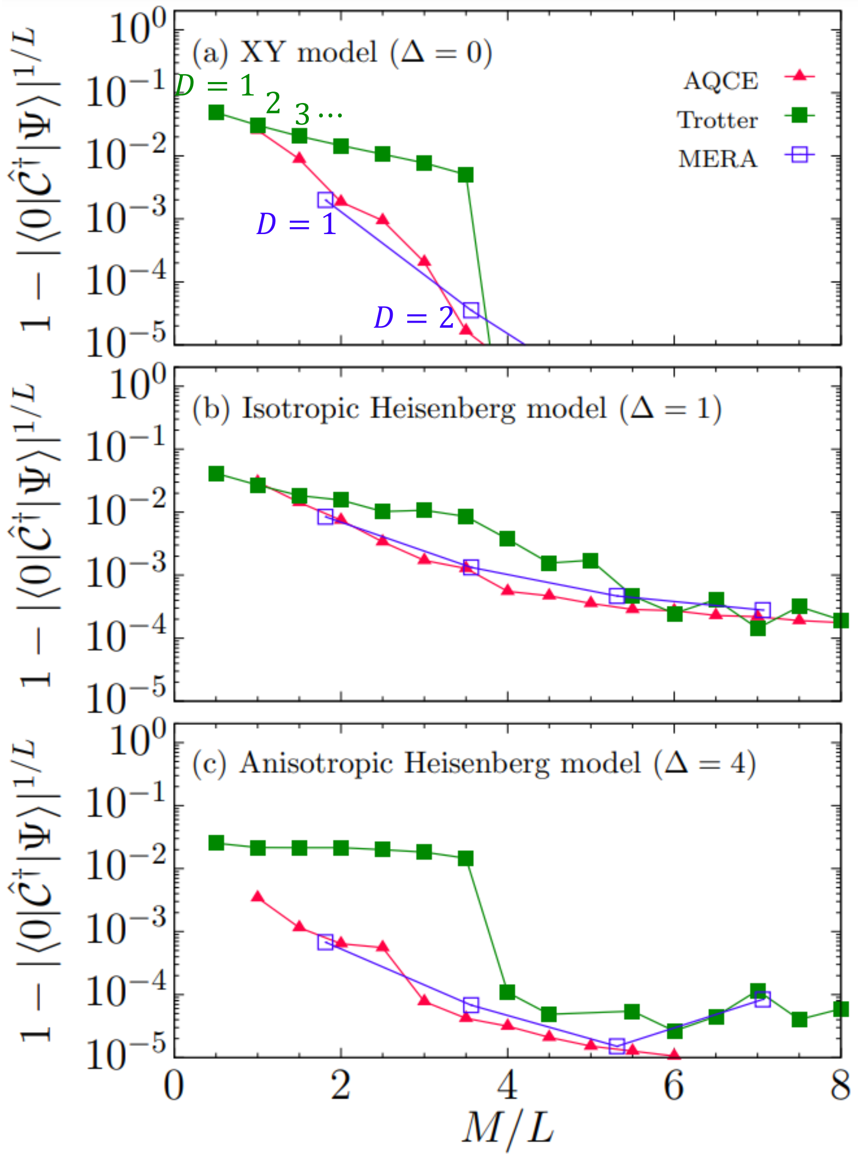

QCE with Fixed Trotter/MERA-like Net.

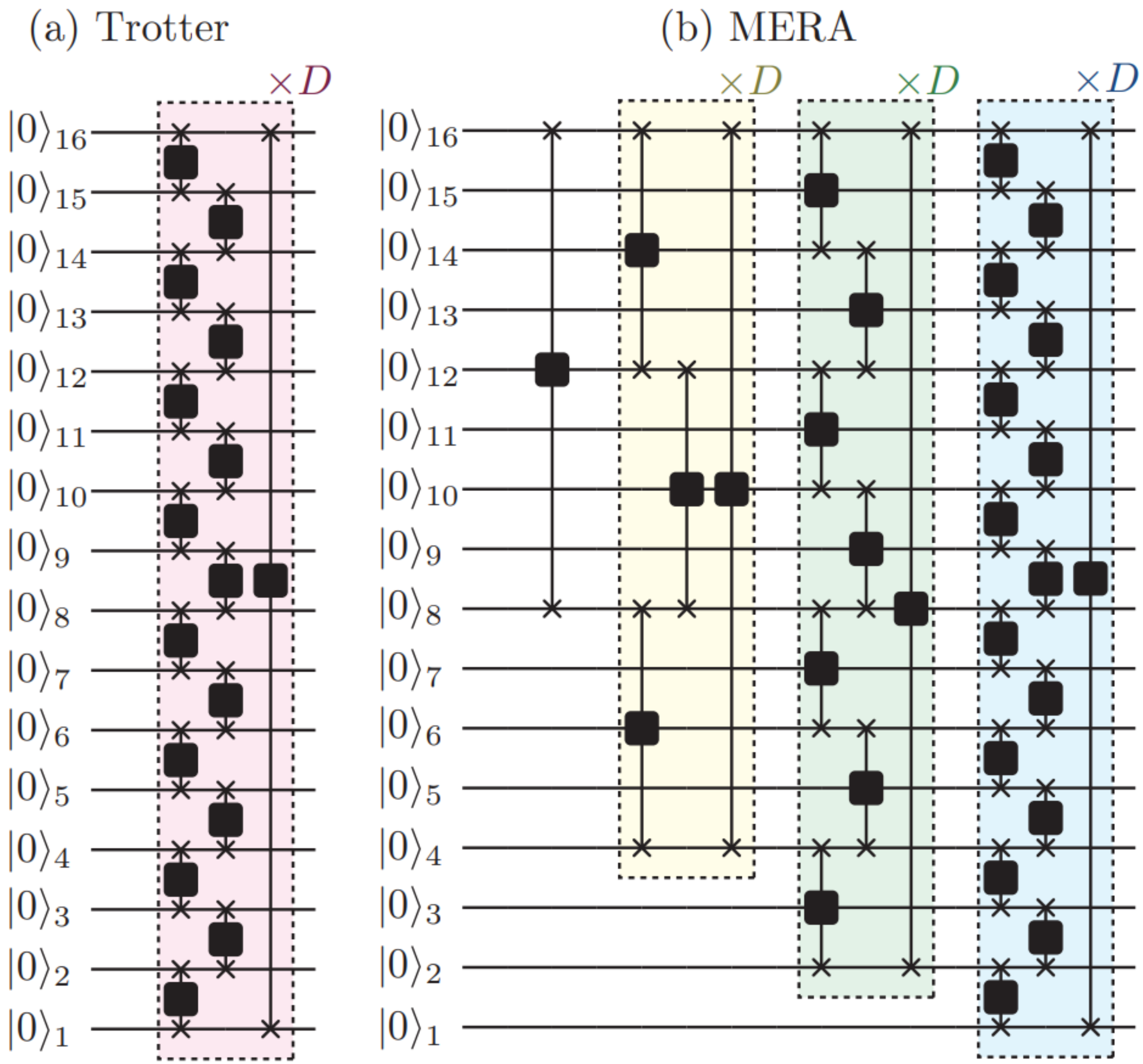

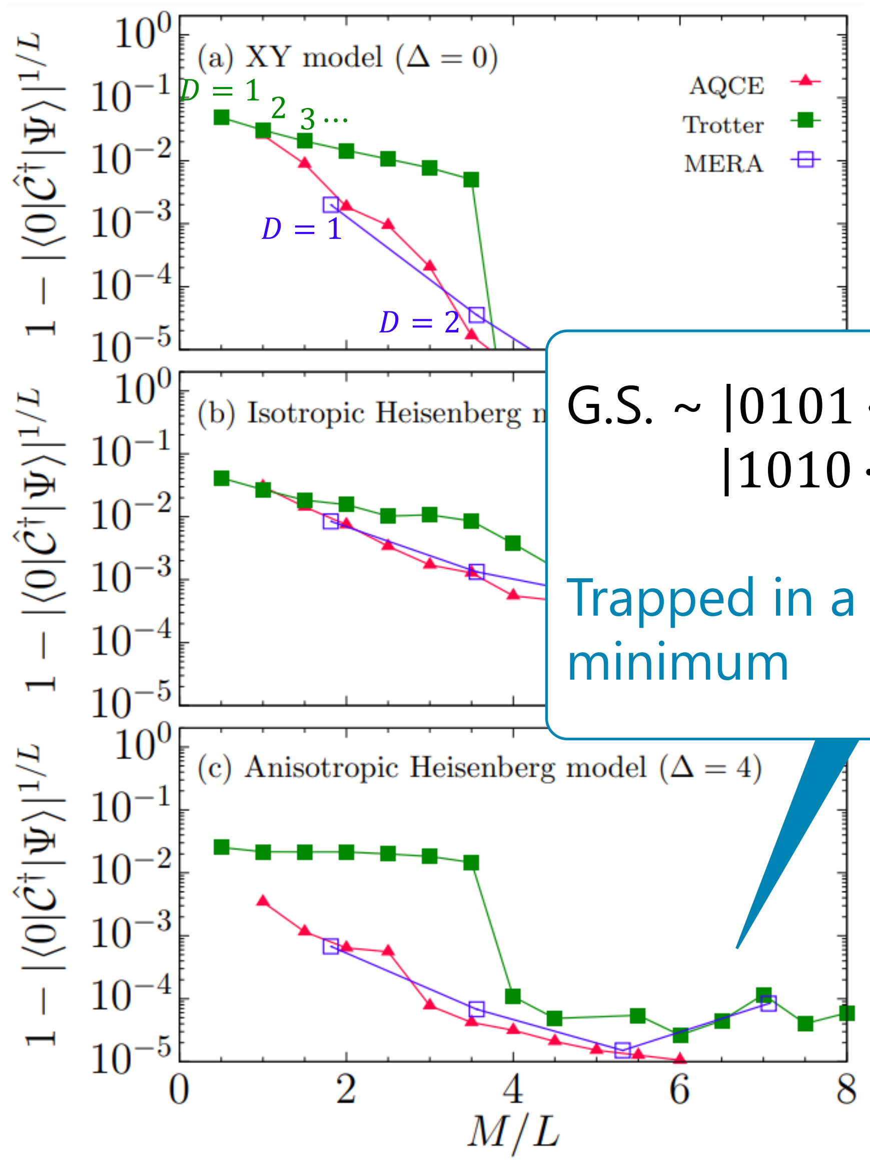

G.S. ~ $|0101\cdots\rangle + |1010\cdots\rangle$

Trapped in a local minimum

Classical data: $\boldsymbol{x}$

$|\Psi_c\rangle = \sum_n \bar{x}_n |n\rangle$

$\bar{x}_n = x_n/\sqrt{V_x}$

$V_x = \sum_n |x_n|^2$

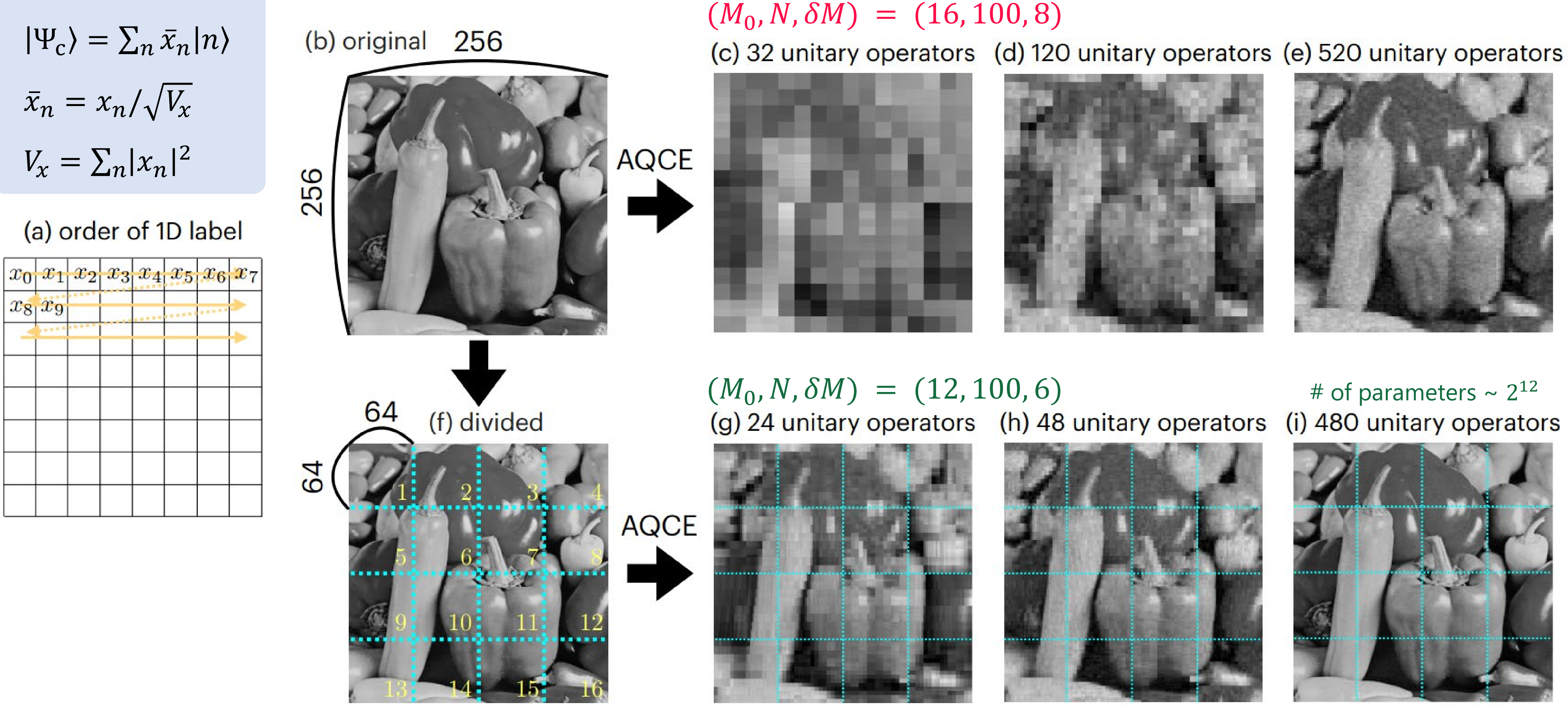

Quantum circuit encoding of classical data

Classical data: $\boldsymbol{x}$

$|\Psi_c\rangle = \sum_n \bar{x}_n |n\rangle$

$\bar{x}_n = x_n/\sqrt{V_x}$

(b) original 256

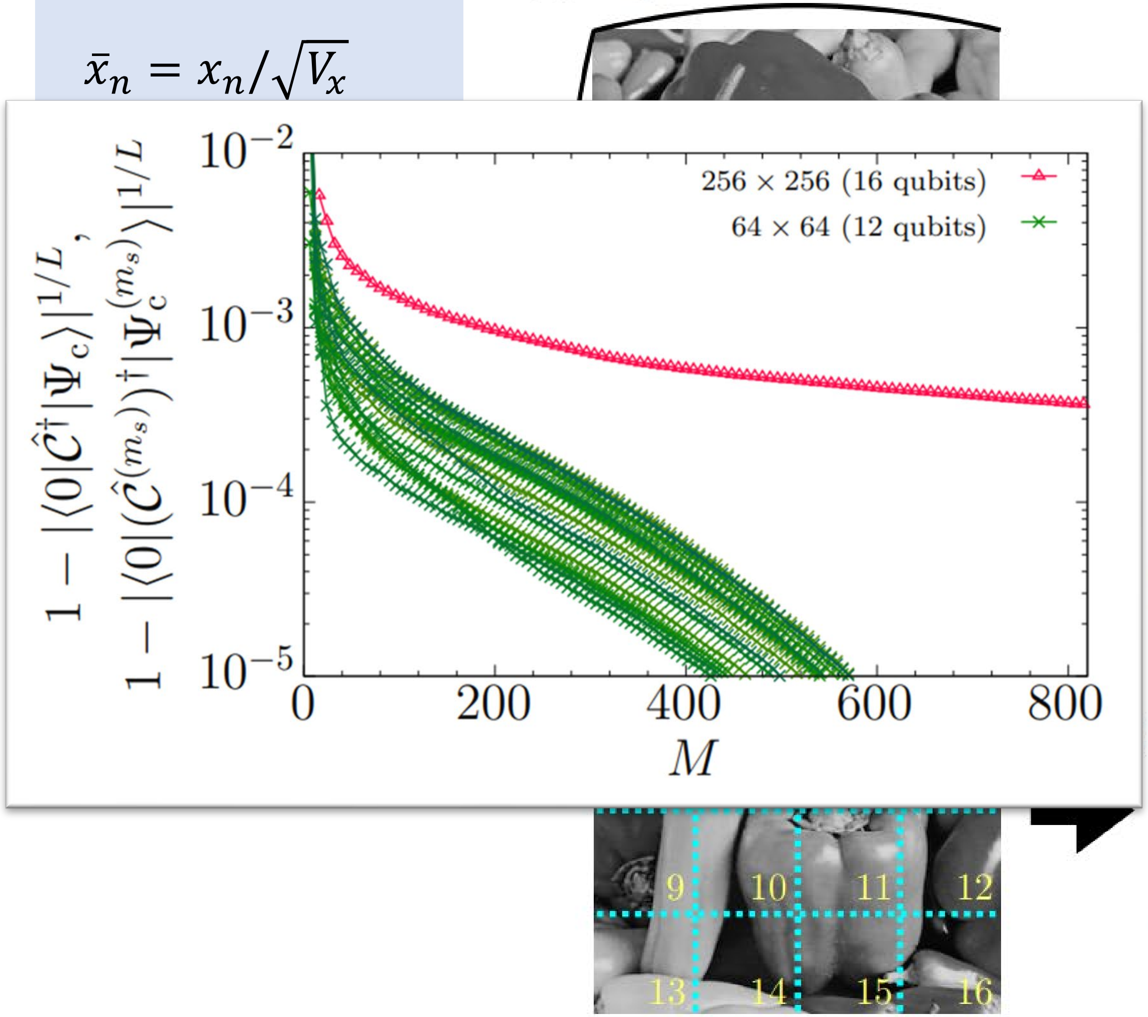

$(M_0, N, \delta M) = (16, 100, 8)$

(c) 32 unitary operators (d) 120 unitary operators (e) 520 unitary operators

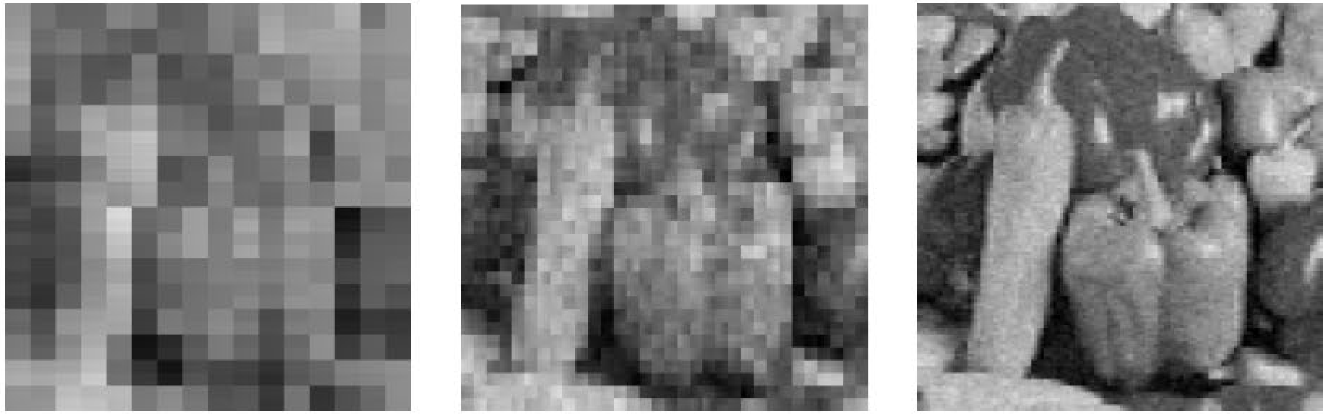

$(M_0, N, \delta M) = (12, 100, 6)$

\# of parameters ~ 2^{12}

(g) 24 unitary operators (h) 48 unitary operators (i) 480 unitary operators

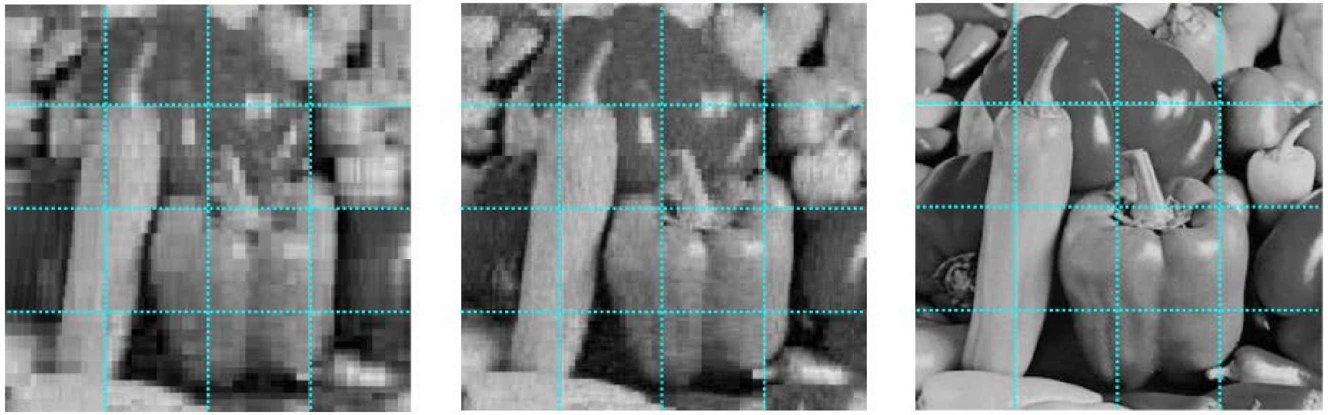

Summary

T. Shirakawa, **HU**, S. Yunoki, arXiv:2112.14524.

- Proposed TN-inspired gradient-free optimization method (AQCE) for Approximate amplitude encoding with $O(\mathrm{poly}(N))$ quantum gates.

- The method, in this talk, consists two-qubit unitary operators
  - ✓Easily generalized for using the K-qubit unitary operators

    Details will be introduced in next divisional meeting!

- Benchmark calculations
  - ✓G.S.s for the XY & Heisenberg model, classical picture, real quantum devices
  - ✓Comparison with QC of fixed TN-like (Trotter, MERA) structures

    AQCE shows good performance irrespective of the details of input data.

最近携わったお仕事一覧

- TNの最適化原理を活用した自動量子回路エンコーディング
  T. Shirakawa, **HU**, S. Yunoki, arXiv: 2112.14524 (2021).
  - TTNの構造探索と最適化
    T. Hikihara, **HU**, K. Okunishi, K. Harada, T. Nishino, Phys. Rev. Res. **5**, 013031 (2023).
    K. Okunishi, **HU**, T. Nishino, PTEP **2023**, 023A02 (2023).

    西野さんの講演
    - MERAの構造探索
      R. Watanabe, **HU**, in preparation.
- TTN構造を使った分割統治VQE
  K. Fujii, K. Mizuta, **HU**, et al., PRX Quantum **3**, 010346 (2022).
- MERA/分岐MERAの構造を活用したTN&VQE相乗フレームワークの拡張
  R. Watanabe, K. Fujii, **HU**, arXiv:2305.06536 (2023).
- TNと直交関数展開を活用した量子状態振幅にエンコードされた関数の抽出
  K. Miyamoto, **HU**, Quantum Inf. Process. **22** 239 (2023).
- ダイヤモンド型量子回路による量子ダイナミクス計算
  S. Miyakoshi, T. Sugimoto, T. Shirakawa, S. Yunoki, **HU**, arxiv:2311.05900 (2023).

Variational state with quantum circuits

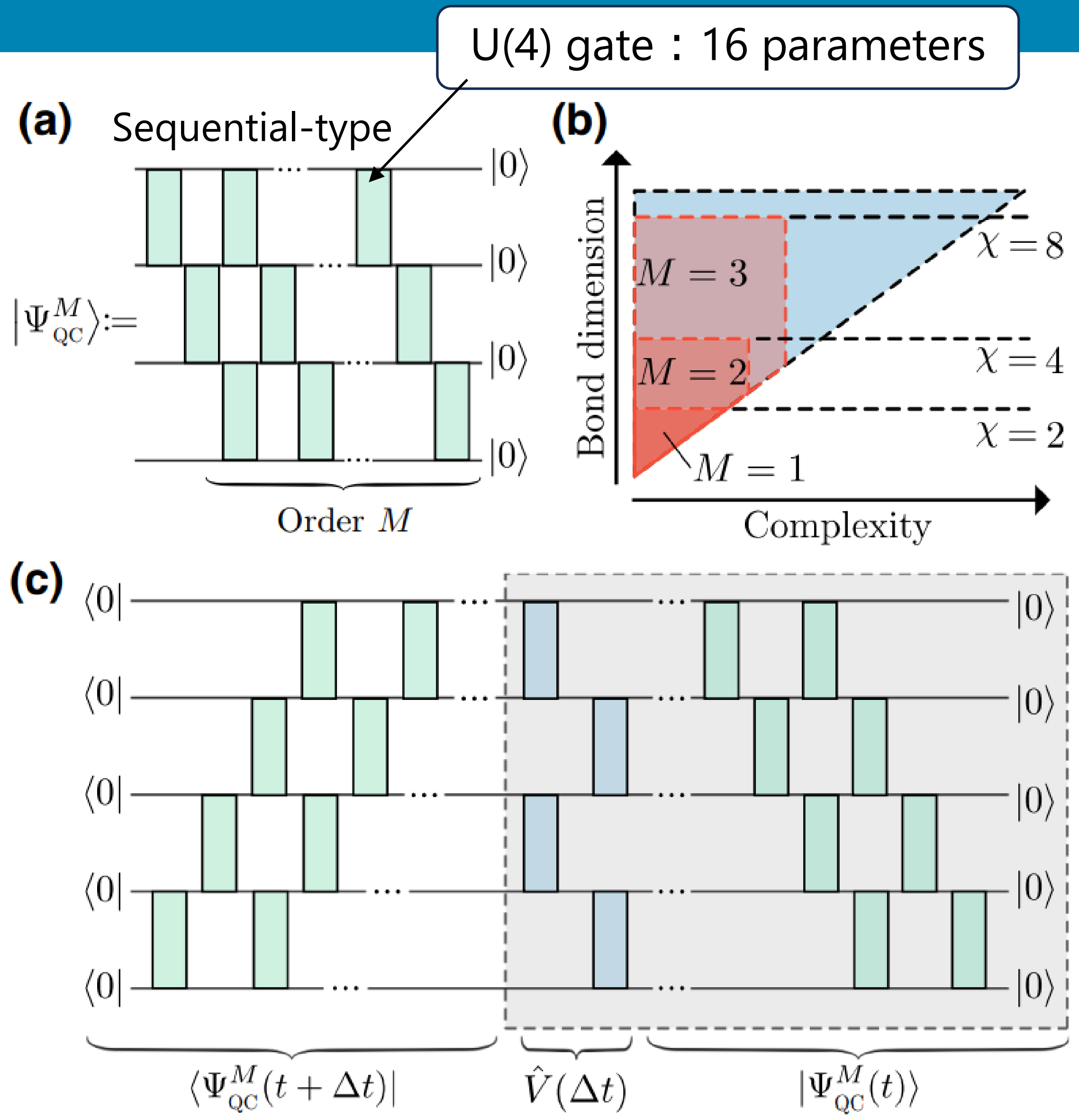

S.-H. Lin et al., PRX Quantum **2**, 010342 (2021).

Hamiltonian:

$$\hat H = -J\left[\sum_{j=1}^{N-1}\hat\sigma^x_j\hat\sigma^x_{j+1} + \sum_{j=1}^{N} g\hat\sigma^z_j + \sum_{j=1}^{N} h\hat\sigma^x_j\right]$$

where

$$\hat\sigma^x_j\hat\sigma^x_{j+1} \doteq \overbrace{\underbrace{I\otimes\cdots\otimes I}_{j-1}\otimes\sigma^x\otimes\sigma^x\otimes I\otimes\cdots\otimes I}^{N}$$

Real-time simulation : $|\Psi(t+\Delta t)\rangle = e^{-i\hat H\Delta t}|\Psi(t)\rangle$
with $|\Psi(0)\rangle = |0\cdots 0\rangle$

Time-evolution operator with a trotter decomposition

$$V(\Delta t) = e^{-i\hat H\Delta t} = e^{-i\hat H_{\rm even}\Delta t/2}e^{-i\hat H_{\rm odd}\Delta t}e^{-i\hat H_{\rm even}\Delta t/2} + O(\Delta t^3)$$

Cost func.: $\mathcal{F} = |\langle\Psi^M_{\rm QC}(t+\Delta t)|\hat V(\Delta t)|\Psi^M_{\rm QC}(t)\rangle|^2$

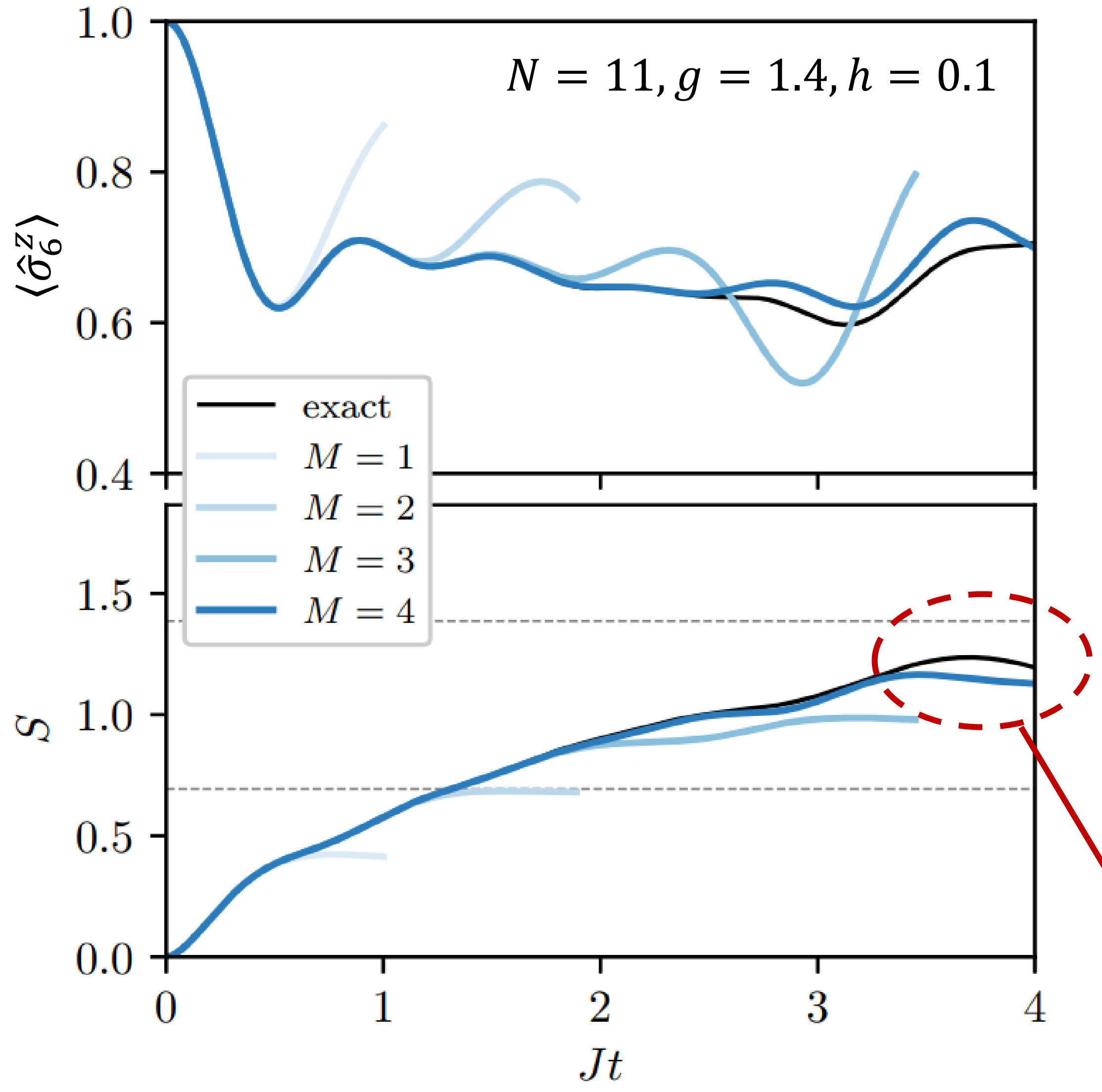

S.-H. Lin et. al., PRX Quantum **2**, 010342 (2021).

Expectation values

$$\langle \hat{\sigma}_j^z \rangle = \langle \Psi_{\mathrm{QC}}^M(t) | \hat{\sigma}_j^z | \Psi_{\mathrm{QC}}^M(t) \rangle$$

Entanglement entropy : S

$$\Psi_{q_1 \cdots q_{N/2}, q_{N/2+1} \cdots q_N} \overset{\mathrm{SVD}}{=} \sum_c u_{q_1 \cdots q_{N/2}, c} \lambda_c v^*_{q_{N/2+1} \cdots q_N, c}$$

$$S = -\sum_c \lambda_c^2 \ln \lambda_c^2$$

How do we describe the large S within a more compact quantum circuit representation?

Rainbow state & Diamond-type QC

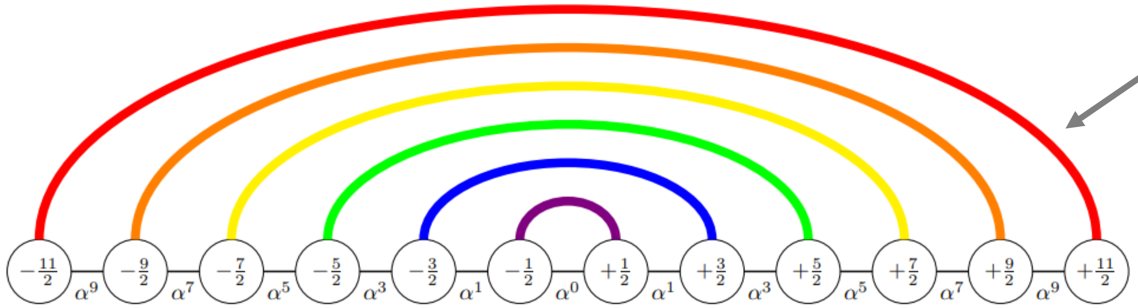

G. Ramírez et al., arXiv:1812.11495

Maximally-entangled state

Ex) $|\psi\rangle_{ij} = \frac{1}{\sqrt{2}}\left(|0\rangle_i|1\rangle_j - |1\rangle_i|0\rangle_j\right)$

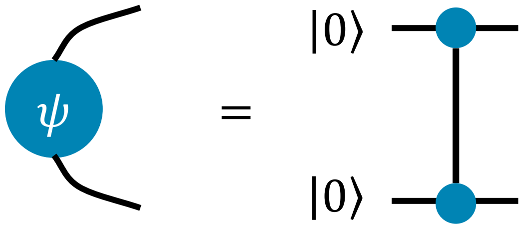

Swap gate

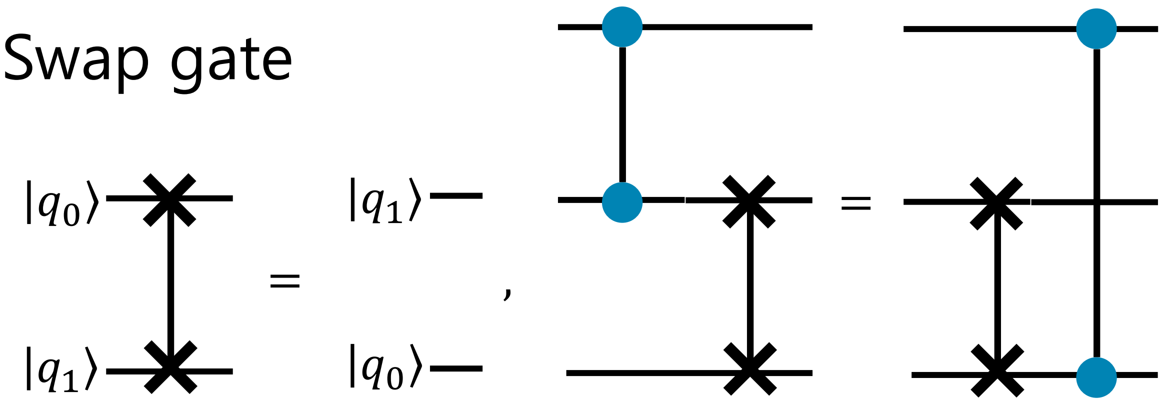

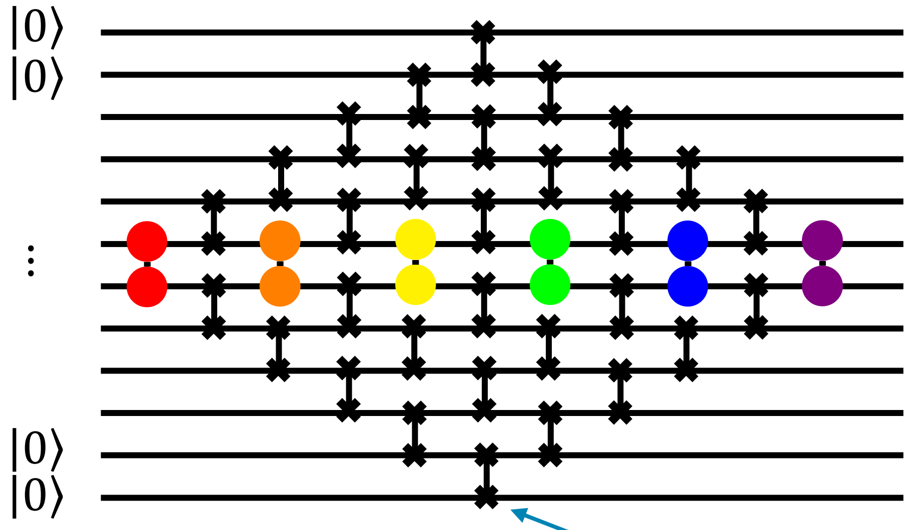

Replace all with U(4) gates for variational state representation

Effective for the transverse-field Ising model

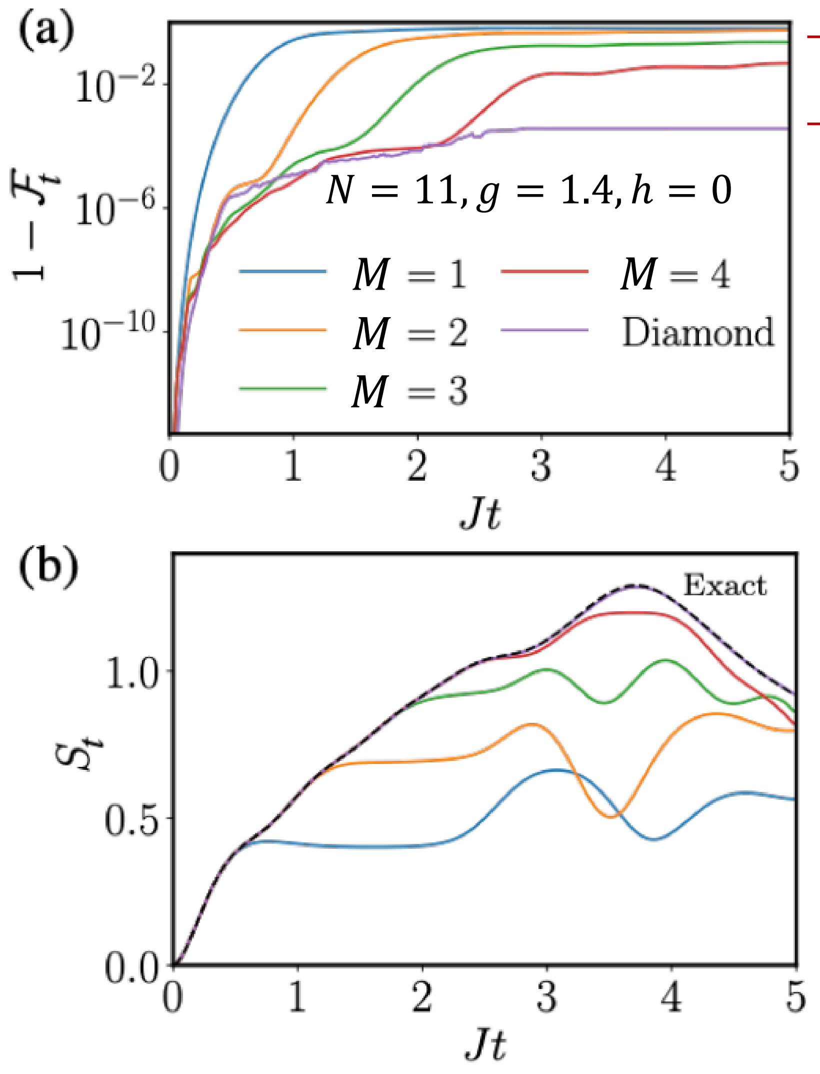

When $N = 11$:

DOF of the diamond-type QC = DOF of the sequential-type QC with $M = 3$.

Fidelity: $\mathcal{F}_t = |\langle \Psi_{\mathrm{exact}}(t) | \Psi_{\mathrm{diamond}}(t) \rangle|^2$

Optimization : Utilizing internal routines in AQCE

T. Shirakawa, **HU**, S. Yunoki, arXiv:2112.14524.

$Jt \geq 3$: Reducing $1 - \mathcal{F}_t$ by a factor of 1/500

Setting the circuit structure based on the system's entanglement structure is extremely important!

S. Miyakoshi, T. Sugimoto, T. Shirakawa, S. Yunoki, and **HU**, arxiv:2311.05900 (2023).

Achieving a numerically exact embedding of the wave function

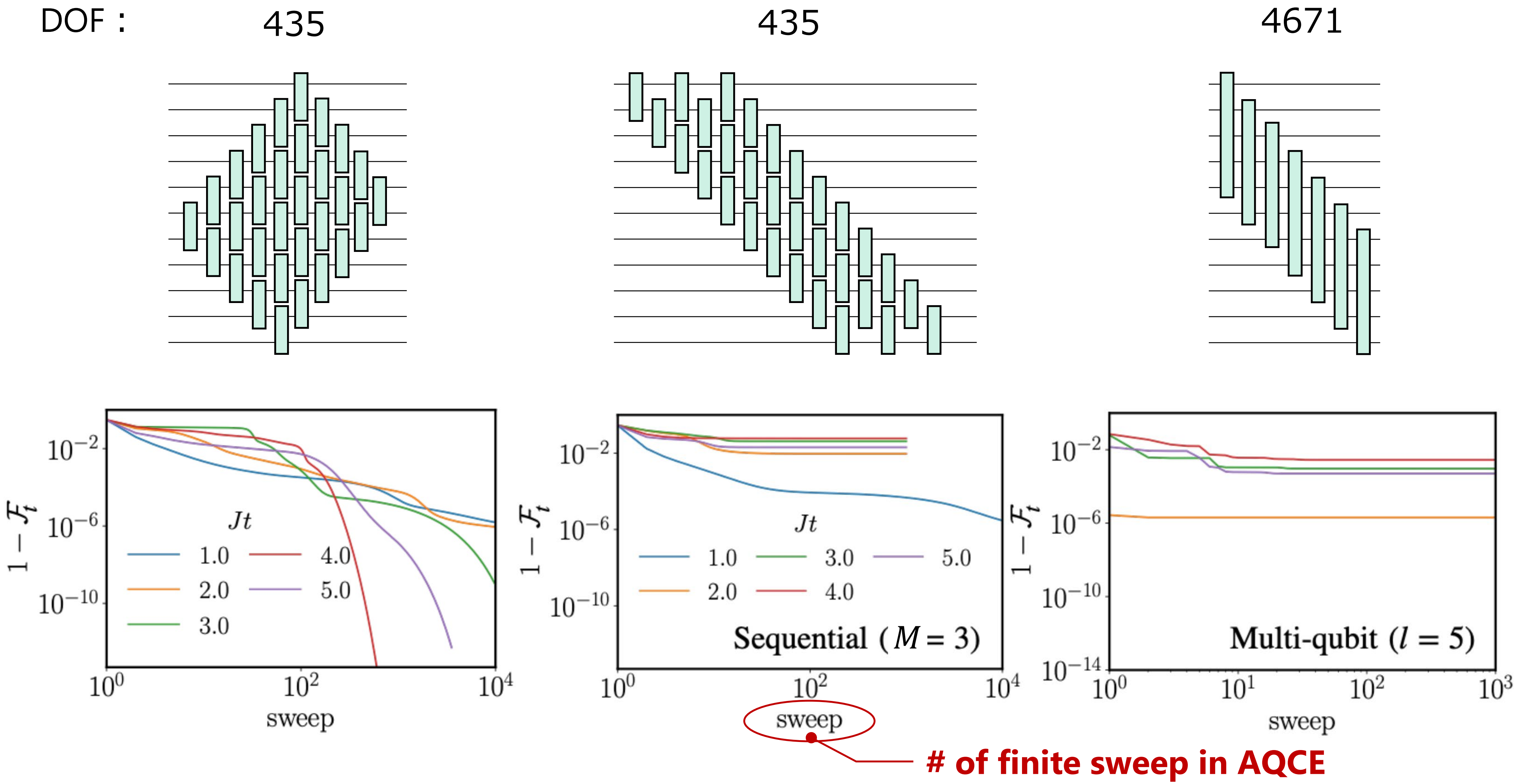

S. Miyakoshi, T. Sugimoto, T. Shirakawa, S. Yunoki, and **HU**, arxiv:2311.05900 (2023).

Strong dependence on the longitudinal magnetic field

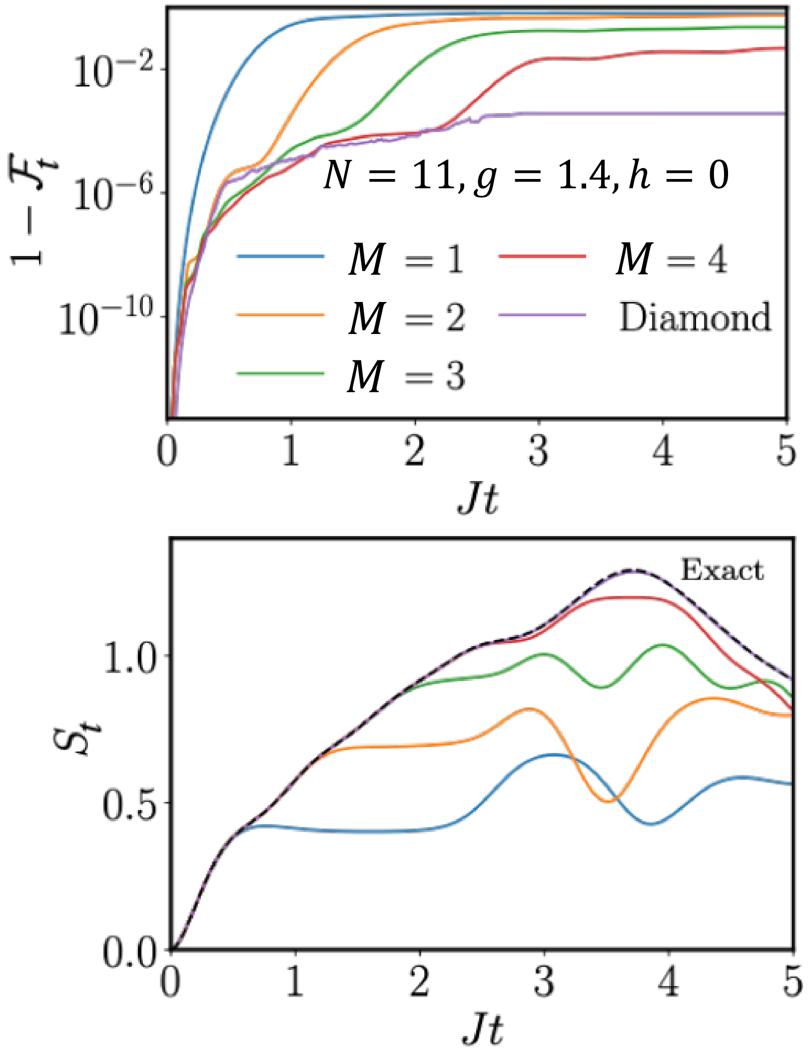

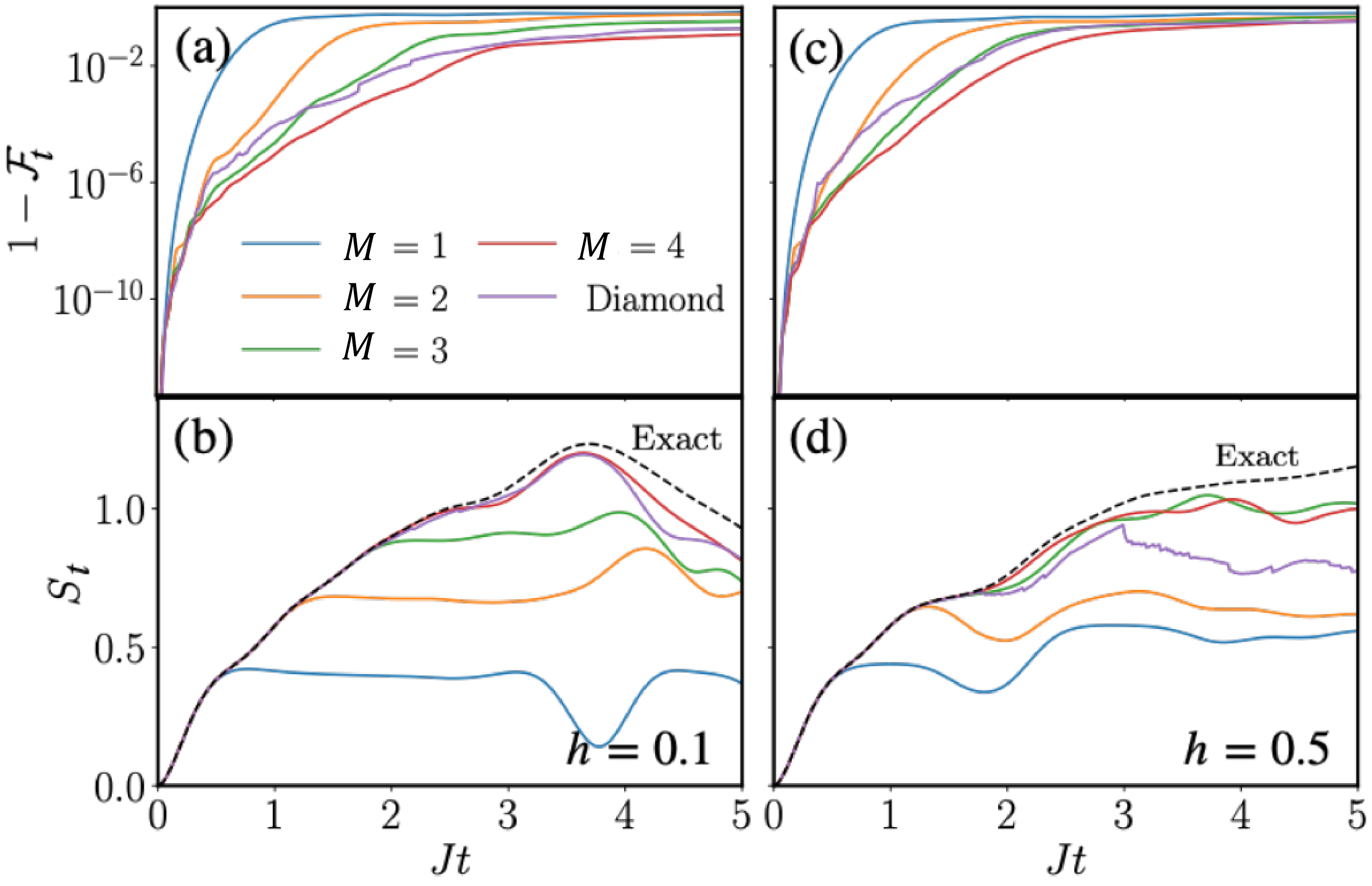

S. Miyakoshi, T. Sugimoto, T. Shirakawa, S. Yunoki, and **HU**, arxiv:2311.05900 (2023).

Effect of quantum scrambling ? PRA **75**, 022304 (2007), PRL **111**, 127205 (2013).

Summary

S. Miyakoshi, T. Sugimoto, T. Shirakawa, S. Yunoki, and HU, arxiv:2311.05900 (2023).

- **Diamond-type: Low-rank tensor decomposition of multi-qubit gates**

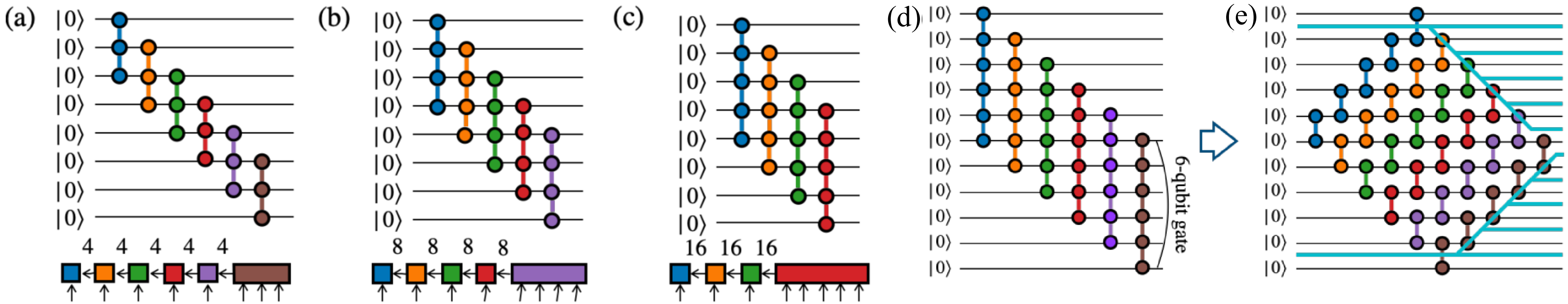

- **Diamond-type ∈ Sequential-type with $M = 5, N = 11$**

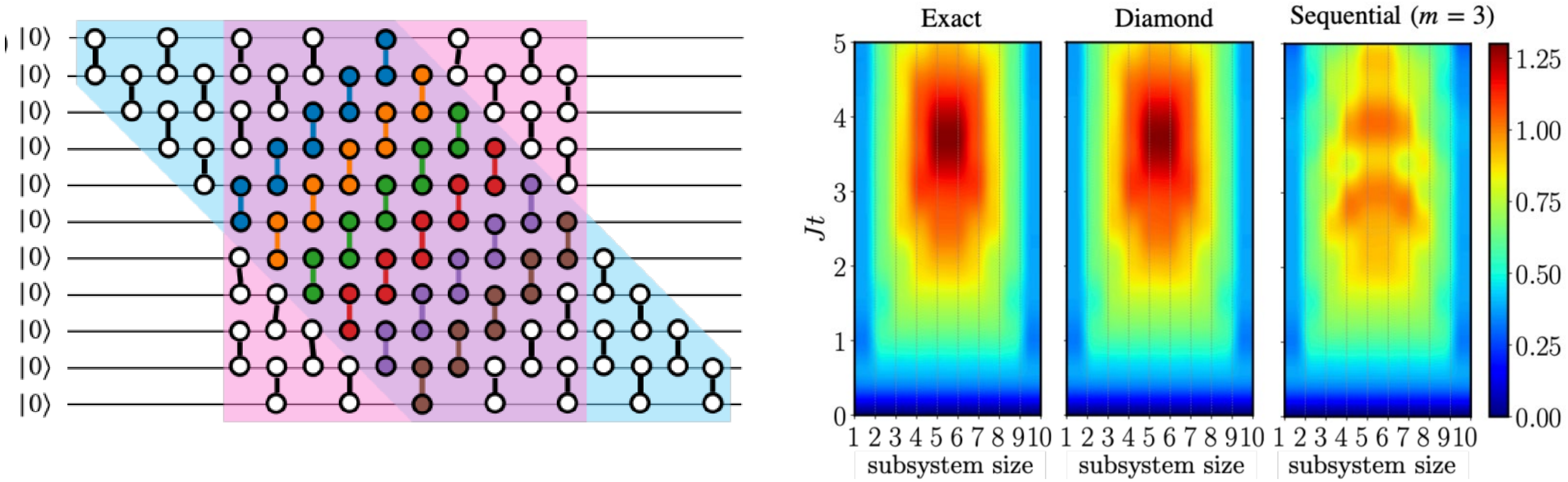

Future issues:
- **In the case of h>0**
- **Higher dimensional systems**

最近携わったお仕事一覧

- TNの最適化原理を活用した自動量子回路エンコーディング
  T. Shirakawa, **<u>HU</u>**, S. Yunoki, arXiv: 2112.14524 (2021).
  - TTNの構造探索と最適化
    T. Hikihara, **<u>HU</u>**, K. Okunishi, K. Harada, T. Nishino, Phys. Rev. Res. **5**, 013031 (2023).
    K. Okunishi, **<u>HU</u>**, T. Nishino, PTEP **2023**, 023A02 (2023).

    西野さんの講演
    - MERAの構造探索
      R. Watanabe, **<u>HU</u>**, in preparation.
- TTN構造を使った分割統治VQE
  K. Fujii, K. Mizuta, **<u>HU</u>**, et al., PRX Quantum **3**, 010346 (2022).
- MERA/分岐MERAの構造を活用したTN&VQE相乗フレームワークの拡張
  R. Watanabe, K. Fujii, **HU**, arXiv:2305.06536 (2023).
- TNと直交関数展開を活用した量子状態振幅にエンコードされた関数の抽出
  K. Miyamoto, **<u>HU</u>**, Quantum Inf. Process. **22** 239 (2023).
- ダイヤモンド型量子回路による量子ダイナミクス計算
  S. Miyakoshi, T. Sugimoto, T. Shirakawa, S. Yunoki, **HU**, arxiv:2311.05900 (2023).

Synergy Between Quantum Circuits and TN

M. S. Rudolph, et al., arXiv:2208.13673.

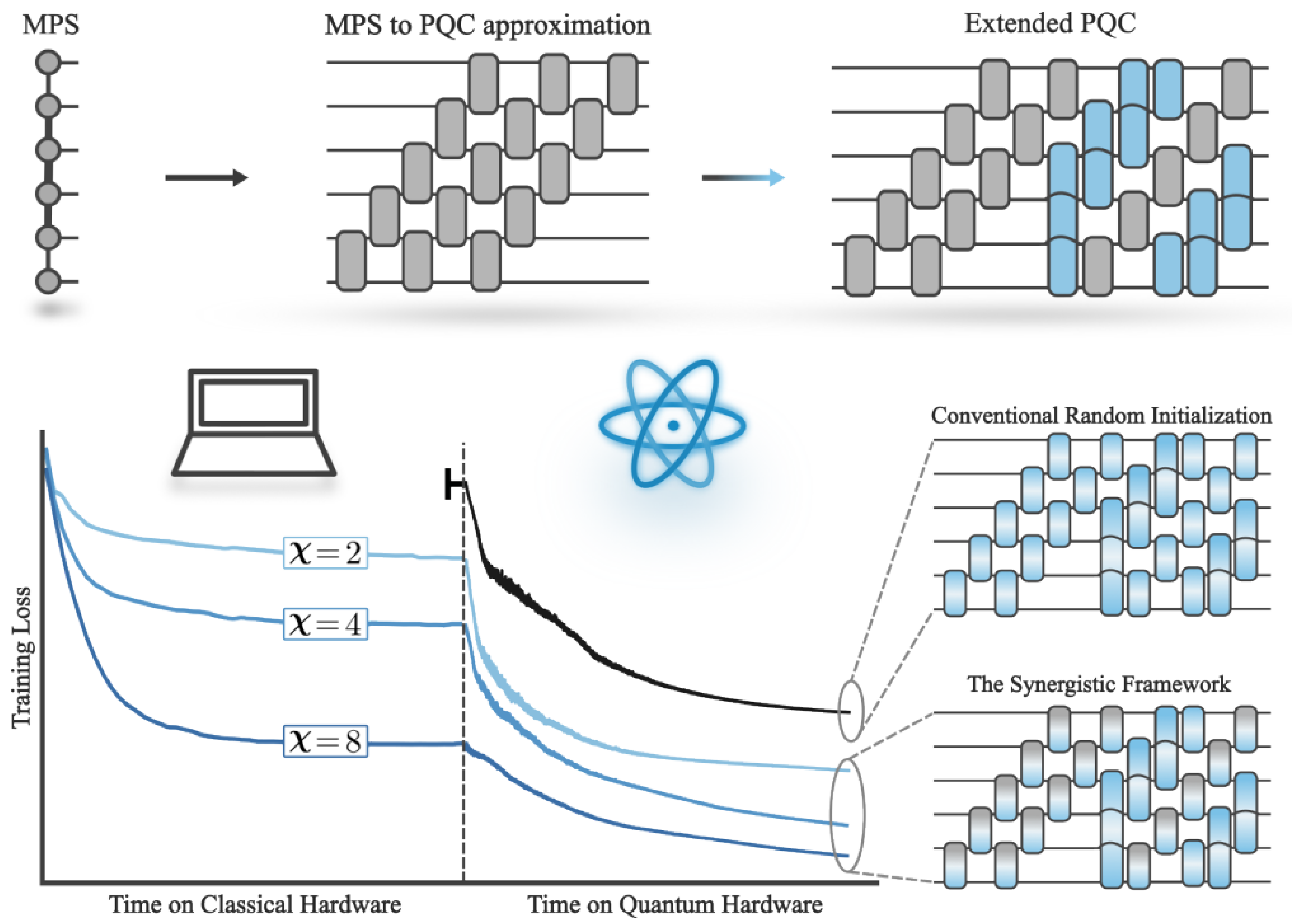

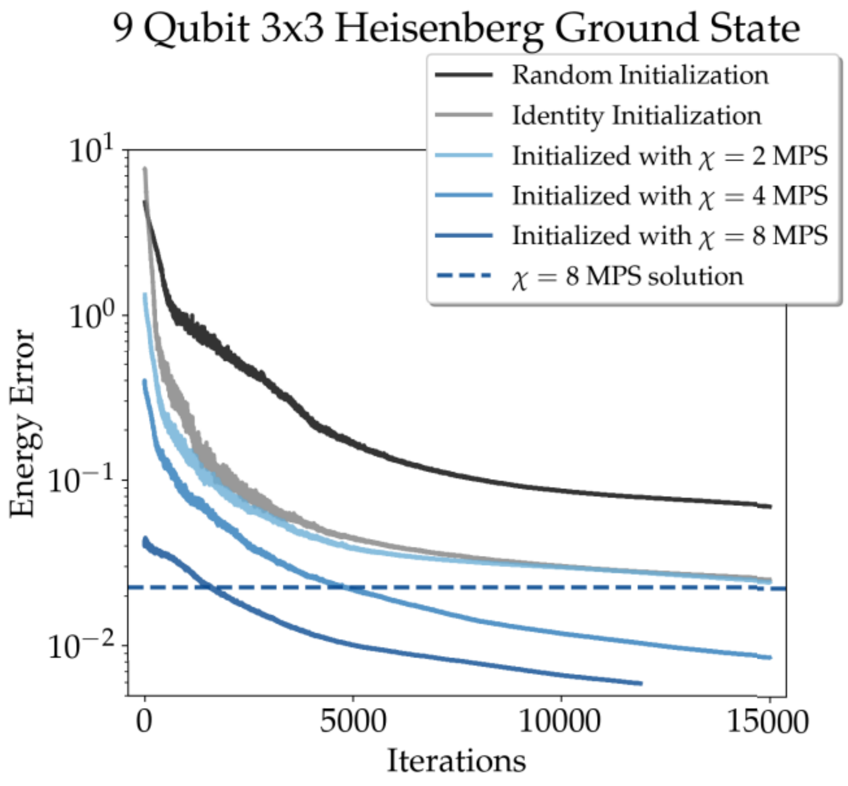

Optimal MPS
+ QC /w all-to-all topology

Entangled embedding VQE with TN

R. Watanabe, K. Fujii, **HU**, arXiv:2305.06536.

Optimized TN (MERA) → QCE of the TN and Effective Entanglement Augmentation → VQE

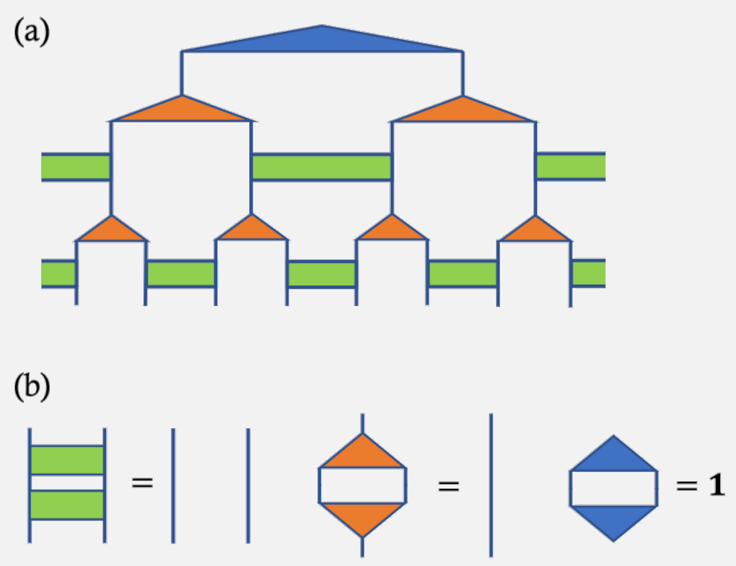

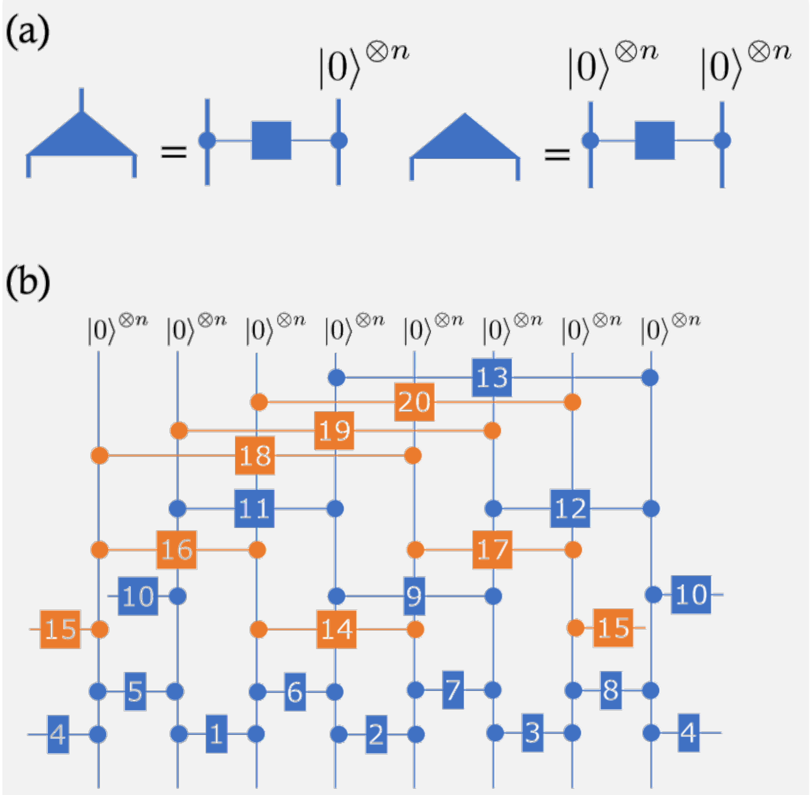

Quantum gates were added during the quantum computation process